

The Pennsylvania State University
The Graduate School
Department of Electrical Engineering

**CHARACTERISTICS OF ATMOSPHERIC WAVES
INFERRED FROM LIDAR MEASUREMENTS**

A Thesis in
Electrical Engineering

by
Byron H. Chen

Submitted in Partial Fulfillment
of the Requirements
for the Degree of
Master of Science

December 1990

We approve the thesis of Byron Chen.

C. Russell Philbrick
Professor of Electrical Engineering
Thesis Advisor

John D. Mathews
Professor of Electrical Engineering

John D. Mitchell
Professor of Electrical Engineering

Larry C. Burton
Professor of Electrical Engineering
Head of the Department Electrical
and Computer Engineering

ABSTRACT

Using a set of data obtained from LIDAR (standing for "light detection and ranging") measurements at $65^{\circ}N$ during February and March 1986 at Poker Flat Research Range, Alaska, an investigation of the planetary and gravity waves in the middle atmosphere has been made. The measurement period included a moderate stratospheric warming which reached its peak response on February 20/21 and the beginning of a major stratospheric warming which started on March 6. The long period variations of the density of the middle atmosphere were modeled by a one-dimensional planetary wave model. The modeled periods of the two principal wave components agree well with the planetary wave numbers 1 and 2. The peak of the density perturbation appears to be due to the sum effects of the constructive interference of the waves. The short period variations of the density were analyzed by spatial spectral estimation. The wave activity at 25-45 km and 45-65 km showed that the level of significant wave breaking had been lowered to below 50 km during the stratospheric warming period.

CONTENTS

LIST OF FIGURES	v
ACKNOWLEDGMENTS	vi
Chapter 1 INTRODUCTION.....	1
Chapter 2 PLANETARY WAVE BACKGROUND.....	5
2.1 The Equation of Motion.....	5
2.2 The Equation of Continuity	10
2.3 The Equation of Two-Dimensional Planetary Waves	10
Chapter 3 SIGNAL PROCESSING BACKGROUND.....	13
3.1 Spectral Estimation.....	13
3.2 Modeling of Data	19
Chapter 4 CHARACTERISTICS OF ATMOSPHERIC WAVES DURING STRATOSPHERIC WARMING PERIODS.....	21
4.1 Characteristics of the Planetary Waves.....	21
4.2 Characteristics of the Gravity Waves	29
Chater 5 CONCLUSIONS.....	34
REFERENCES	36
Appendix COMPUTER PROGRAMS.....	38

LIST OF FIGURES

1. Density ratio as a function of date	2
2. Temperature as a function of date.....	3
3. Set of axes at any point on the earth's surface.....	7
4. The elementary volume	7
5. Comparison of the results from two spectral estimators:	
(a) Blackman-Tukey	23
(b) Maximum Entropy	23
6. Spectral estimation by MEM at all altitudes	25
7. Modeled density variations.....	26
8. Comparison of the modeled densities and the measured	27
9. Phase shift of the two principal wave components	28
10. Gravity wave activity at different altitude ranges during stratospheric warming periods:	
(a) Feb. 18-22	30
(b) Mar. 4-8	31
11. Mean zonal wind and temperature differences in the winter of 1986:	
(a) mean zonal wind at $60^{\circ}N$	32
(b) temperature differences between $60^{\circ}N$ and the pole.....	32

Chapter 1

INTRODUCTION

The structure profiles in the middle atmosphere are known to be frequently and considerably disturbed in the northern winter (Philbrick et al. 1985). LIDAR sounding from the ground offers the new possibility of studying the characteristics of wave propagation in the profiles of density and temperature for examining the consequences of the dynamical processes in the middle atmosphere.

From February 14 to March 9, 1986, the density perturbations in the high latitude middle atmosphere were measured continuously by LIDAR (standing for “light detection and ranging”) at the Poker Flat Research Range near Fairbanks, Alaska (Philbrick et al. 1987a and 1987b).

The full night mean density profiles are shown in Figure 1 and mean temperature profiles are shown in Figure 2. Clearly, there was a large perturbation of density at the altitude of 40 – 50 km which reaches a maximum on February 21. This perturbation corresponds to a period of moderate stratospheric warming and appears to correlate with the constructive interference, or the superposition of planetary waves. It corresponds, as well, to a period of extreme wave activity in the stratosphere and cessation of gravity wave activity in the mesosphere.

Naujokat and Labitzke (1986) have reported the stratospheric warming about the same time and latitude but based on the satellite data. The dynamical behavior of the middle atmosphere during a stratospheric warming has been studied by various authors, for instance, Offermann et al. (1987), McIntyre and Palmer (1983), Haynes and McIntyre (1986), Holton (1982), Salby (1984), etc. In this thesis, emphases are placed on the characteristics of the planetary waves and gravity waves

2

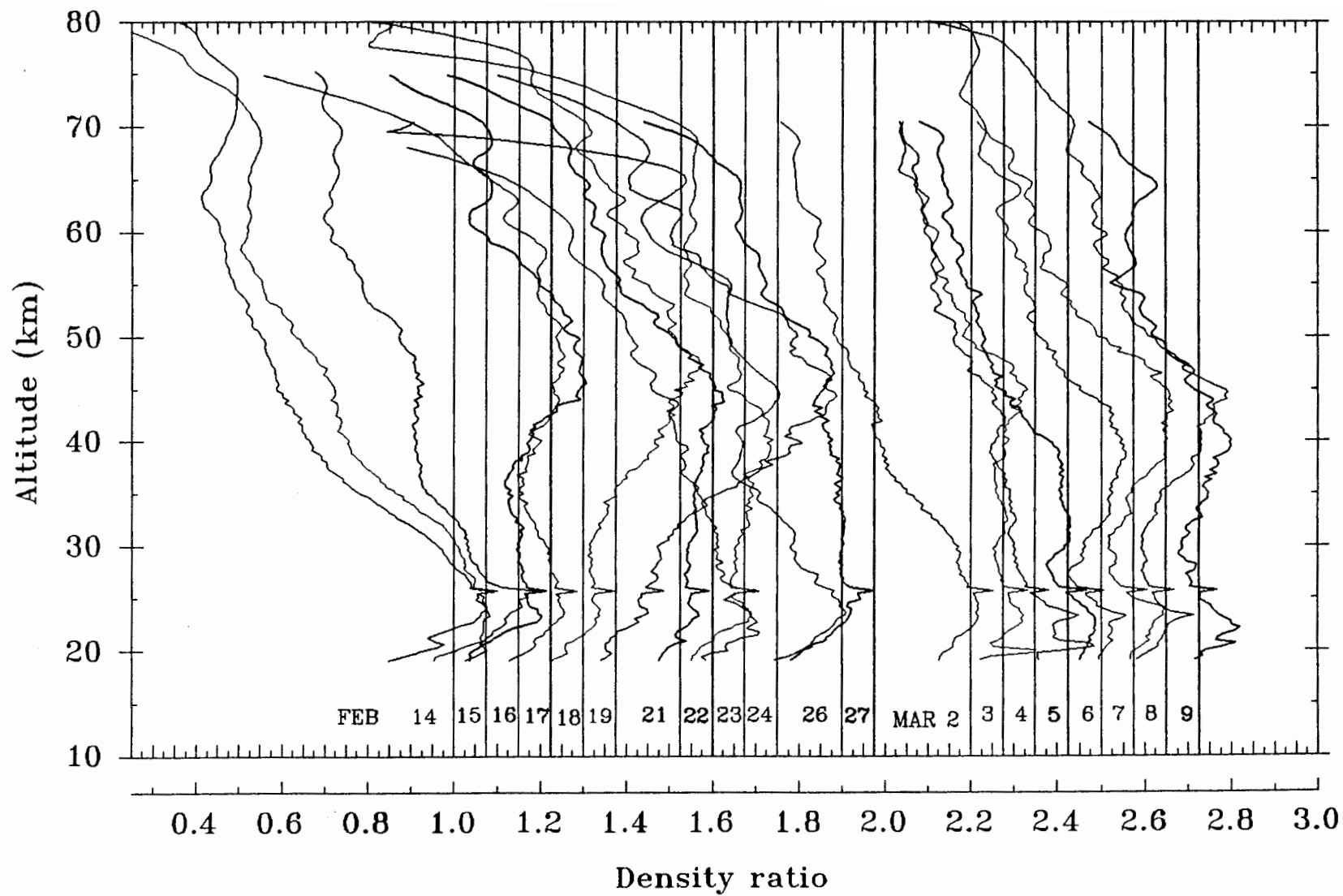


Fig. 1 Density ratio as a function of date

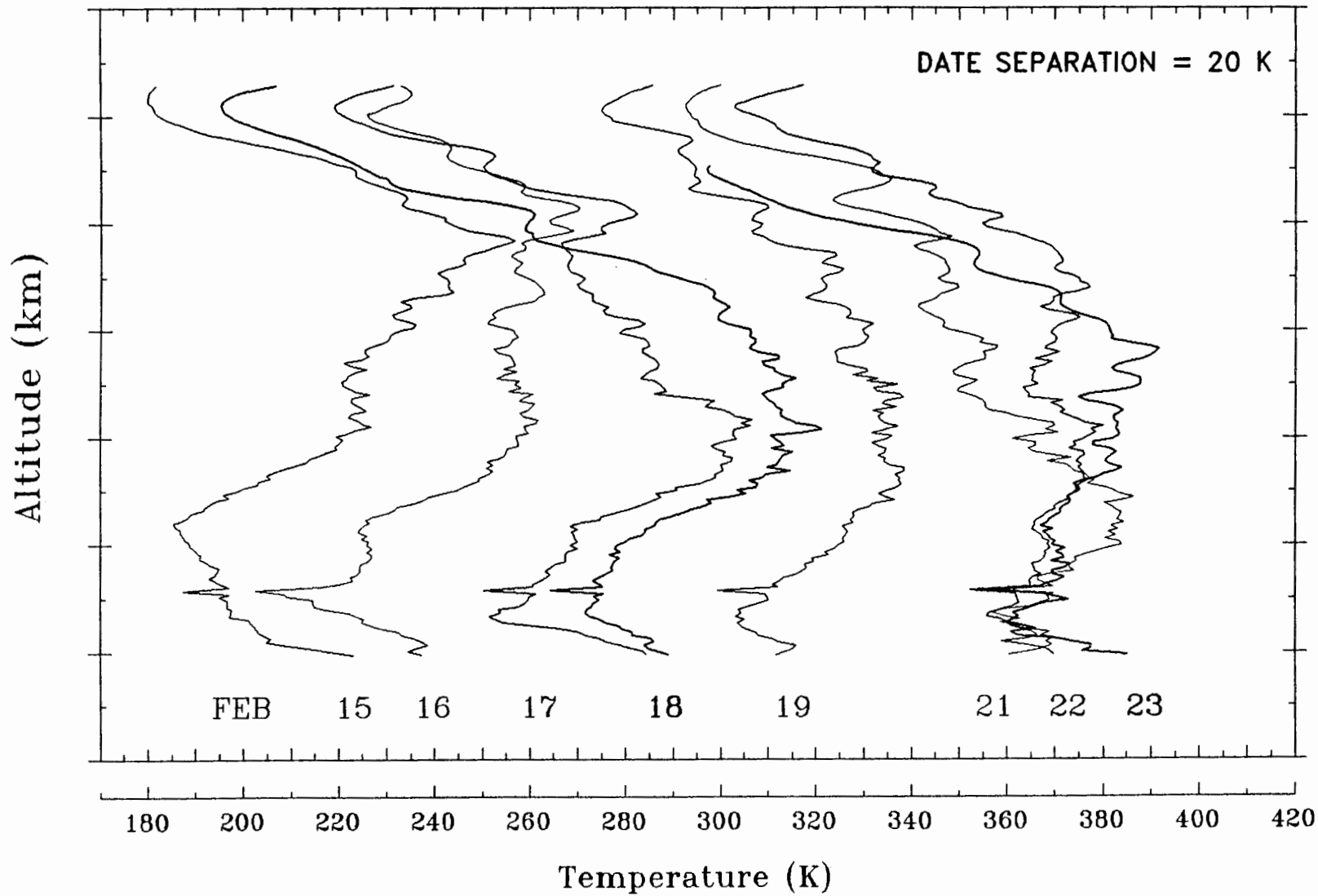


Fig. 2. Temperature as a function of date

during a stratospheric warming. Chapter 2 presents a brief description of the background in planetary waves. Chapter 3 is devoted to a description of the methods of signal processing involved in the analysis. In Chapter 4, a model of planetary waves has been developed to demonstrate the characteristics of the principle planetary wave components. In order to reduce the number of the parameters to be determined in the model, different power spectral estimators were tried in an effort to pick the major frequency components. Then a monotonic spatial power spectral estimation was applied to the density signals with short periods, which are normally associated with the gravity waves. The spatial spectral estimation was carried out at different altitude ranges. The results show that, in the stratosphere, there was strong short period wave activity during the stratospheric warming periods, while in the mesosphere, the wave activity was much weaker when compared to the usual case.

Chapter 2

PLANETARY WAVE BACKGROUND

The very large scale wave features which are observed in the flow on the planetary scales are known as planetary waves. Those waves that owe their existence to the variation of the Coriolis force with latitude are known as Rossby waves. The characteristics of those waves during the stratospheric warming periods in 1986 have been investigated based on the measurements of a LIDAR. To provide a background of this aspect, a review of the derivation of equation of motion, equation of continuity and equations of planetary waves is presented in this chapter (Houghton 1986, pp. 88-113; Holton 1979, pp. 27-44 and pp. 147-167).

2.1 The Equation of Motion

By Newton's second law of motion ($M\vec{a} = \sum_i \vec{f}_i$), the equation of motion for an element of fluid of density ρ moving with velocity \vec{v} in the presence of a pressure gradient ∇p and a gravitational field \vec{g} is

$$\frac{d\vec{v}}{dt} = \vec{g} - \frac{1}{\rho} \nabla p + \vec{F}, \quad (2.1)$$

where \vec{F} is the frictional force on the element. Note that, for a motion with a scale large enough as compared to the radius of the earth, equation (2.1) applies to an inertial frame of reference, i.e., fixed with respect to the solar system. We are interested, however, only in the motion of the element that is relative to axes fixed with respect to the earth's surface, not that of the sun. Hence the angular velocity $\vec{\Omega}$ of the earth has to be taken into account in equation (2.1).

Denoting 'e' the frame that is rotating at angular velocity $\vec{\Omega}$ with respect to the sun and 's' the frame that is fixed to the sun. The velocities of the element in those two frames have the following relation

$$\left(\frac{d\vec{r}}{dt}\right)_s = \left(\frac{d\vec{r}}{dt}\right)_e + \vec{\Omega} \times \vec{r}, \quad (2.2a)$$

where \vec{r} is a radius vector, or

$$\vec{v}_s = \vec{v}_e + \vec{\Omega} \times \vec{r}, \quad (2.2b)$$

where \vec{v}_s is the velocity of the element in frame s while \vec{v}_e the velocity in frame e. Likewise, the relation of the accelerations in the two frames is

$$\begin{aligned} \left(\frac{d\vec{v}_s}{dt}\right)_s &= \left(\frac{d\vec{v}_s}{dt}\right)_e + \vec{\Omega} \times \vec{v}_s \\ &= \left(\frac{d(\vec{v}_e + \vec{\Omega} \times \vec{r})}{dt}\right)_e + \vec{\Omega} \times (\vec{v}_e + \vec{\Omega} \times \vec{r}) \\ &= \frac{d\vec{v}_e}{dt} + 2\vec{\Omega} \times \vec{r} + \vec{\Omega} \times \vec{v}_e. \end{aligned} \quad (2.3)$$

Substituting equation (2.3) in equation (2.1), yields

$$\frac{d\vec{v}}{dt} = 2\vec{v} \times \vec{\Omega} - \frac{1}{\rho} \nabla p + \vec{g} + \vec{F}, \quad (2.4)$$

where $\vec{v} = \vec{v}_e$ and $\vec{g} = \vec{g}' - \vec{\Omega} \times (\vec{\Omega} \times \vec{r})$ is the acceleration due to the gravity and the centrifugal term $\vec{\Omega} \times (\vec{\Omega} \times \vec{r})$. The first term on the right-hand side is the so-called Coriolis force which applies particularly to the moving element in rotating frames.

To obtain the component equations in cartesian coordinates, assuming a set of axes at any point on the earth's surface (see Figure 3) having x directed towards the east, y west and z vertically upwards, the velocity vector is written

$$\vec{v} = \vec{i}u + \vec{j}v + \vec{k}w \quad (2.5)$$

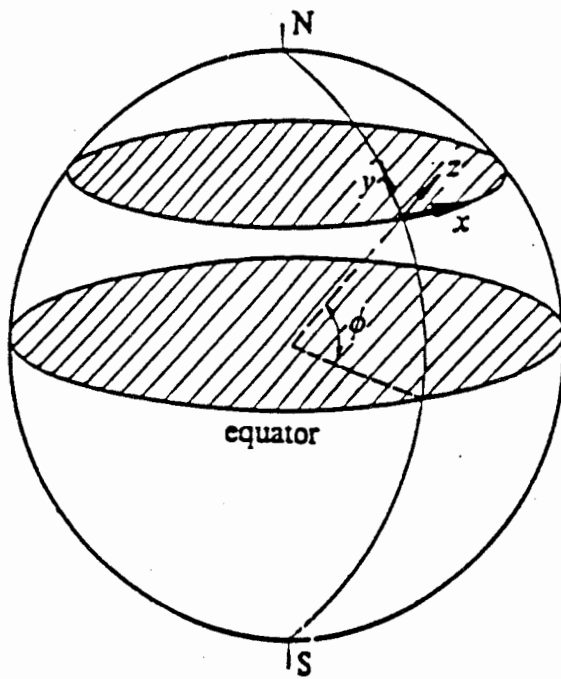


Fig. 3. Set of axes at any points on the earth's surface

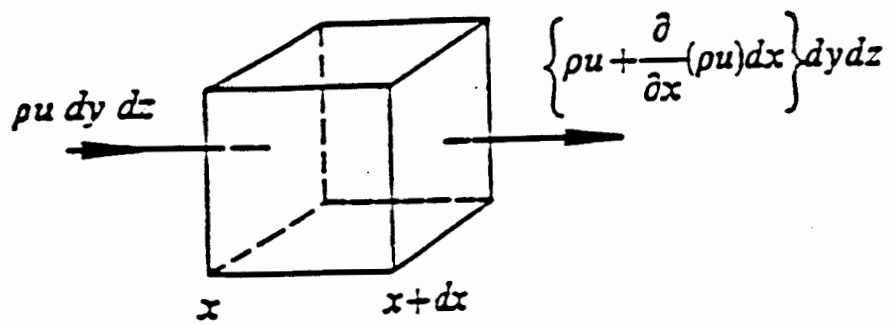


Fig. 4. The elementary volume

where u, v and w are the components of the velocity \vec{v} in the x, y, z directions respectively and $\vec{i}, \vec{j}, \vec{k}$ are unit vectors directed along each axes, as shown in Figure 3.

Obviously, the directions of the axes (i.e., the unit vectors \vec{i}, \vec{j} and \vec{k}) in Figure 3 are changing with position. In other words, those unit vectors are functions of x, y and z . The total derivative therefore of \vec{v} in equation (2.5) is

$$\begin{aligned} \frac{d\vec{v}}{dt} &= \left(\vec{i} \frac{du}{dt} + \vec{j} \frac{dv}{dt} + \vec{k} \frac{dw}{dt} \right) + \left(u \frac{d\vec{i}}{dt} + v \frac{d\vec{j}}{dt} + w \frac{d\vec{k}}{dt} \right) \\ &= \left(\frac{du}{dt} - \frac{uv \tan \phi}{a} + \frac{uw}{a} \right) \vec{i} \\ &\quad + \left(\frac{dv}{dt} + \frac{u^2 \tan \phi}{a} + \frac{vw}{a} \right) \vec{j} \\ &\quad + \left(\frac{dw}{dt} - \frac{u^2 + v^2}{a} \right) \vec{k}, \end{aligned} \quad (2.6)$$

where a is the radius of the earth and ϕ is the latitude. Since $\vec{\omega}$ has no component parallel to \vec{i} and its components parallel to \vec{j} and \vec{k} are $\Omega \cos \phi$ and $\Omega \sin \phi$, respectively, the vector cross product

$$\begin{aligned} 2\Omega \times \vec{v} &= 2\Omega \begin{vmatrix} \vec{i} & \vec{j} & \vec{k} \\ 0 & \cos \phi & \sin \phi \\ u & v & w \end{vmatrix} \\ &= (2\Omega w \cos \phi - 2\Omega v \sin \phi) \vec{i} + 2\Omega u \sin \phi \vec{j} - 2\Omega u \cos \phi \vec{k}. \end{aligned} \quad (2.7)$$

The pressure gradient force can be expressed as

$$\nabla p = \vec{i} \frac{\partial p}{\partial x} + \vec{j} \frac{\partial p}{\partial y} + \vec{k} \frac{\partial p}{\partial z}. \quad (2.8)$$

The gravity can be represented as

$$\vec{g} = -g \vec{k}, \quad (2.9)$$

and friction can be expanded as

$$\vec{F} = \vec{i} F_x + \vec{j} F_y + \vec{k} F_z. \quad (2.10)$$

Substituting (2.6)-(2.10) in (2.4) and equating all terms in the \vec{i}, \vec{j} and \vec{k} directions, respectively, we obtain the eastward, northward and vertically upward component equations,

$$\frac{du}{dt} - \frac{uv \tan \phi}{a} + \frac{uw}{a} = -\frac{1}{\rho} \frac{\partial p}{\partial x} + 2\Omega v \sin \phi - 2\Omega w \cos \phi + F_x, \quad (2.11)$$

$$\frac{dv}{dt} + \frac{u^2 \tan \phi}{a} + \frac{vw}{a} = -\frac{1}{\rho} \frac{\partial p}{\partial y} - 2\Omega u \sin \phi + F_y, \quad (2.12)$$

$$\frac{dw}{dt} - \frac{u^2 + v^2}{a} = -\frac{1}{\rho} \frac{\partial p}{\partial z} - g + 2\Omega u \cos \phi + F_z. \quad (2.13)$$

The magnitudes of the various terms in the above equations will be very different, depending on the scale of the motion under study. Here we shall be concerned with motions on what is generally known as the synoptic scale, that is, systems of typically 1000 km in horizontal dimension, very much larger than their vertical scale (of order 1 scale height or ~ 10 km). For this scale observed vertical velocities (typically 1 cm s^{-1}) are very much smaller than than horizontal velocities (typically 10 m s^{-1}), so that in equation (2.11)-(2.13) terms involving w can be neglected. Again, because those terms in the equation involving a in the denominator are smaller by about one order of magnitude than the other terms and may therefore be neglected, the momentum equations (2.11)- (2.13) thus may be simplified as

$$\begin{aligned} \frac{du}{dt} + \frac{1}{\rho} \frac{\partial p}{\partial x} &= 2\Omega v \sin \phi \\ \frac{dv}{dt} + \frac{1}{\rho} \frac{\partial p}{\partial y} &= -2\Omega u \sin \phi \\ \frac{dw}{dt} + \frac{1}{\rho} \frac{\partial p}{\partial z} + g &= 2\Omega u \cos \phi, \end{aligned} \quad (2.14)$$

where friction force \vec{F} is neglected.

2.2 The Equation of Continuity

The equation of continuity states that the net flow of mass into unit volume per unit time is equal to the local rate of change of density.

In the elementary volume (Figure 4) where the density is ρ and u , v and w are the velocity components along Cartesian axes, the mass entering the volume per unit time at x over the face of area $dydz$ is $\rho dydz$, and leaving at $x + dx$ is $(\rho u + \frac{\partial(\rho u)}{\partial x} dx) dydz$. Thus the net rate of flow into the volume due to the x velocity component is $-\frac{\partial(\rho u)}{\partial x} dx dydz$. Adding x , y and z components together, we have

$$\frac{\partial(\rho u)}{\partial x} + \frac{\partial(\rho v)}{\partial y} + \frac{\partial(\rho w)}{\partial z} = -\frac{\partial \rho}{\partial t}. \quad (2.15)$$

For an incompressible fluid the above equation reduces to

$$\frac{\partial u}{\partial x} + \frac{\partial v}{\partial y} + \frac{\partial w}{\partial z} = 0. \quad (2.16)$$

It was shown through scale analysis that for purely horizontal flow the atmosphere behaves as though it were an incompressible fluid (Holton 1979. pp. 43-44).

2.3 The Equation of Two-Dimensional Planetary Waves

Assuming there is no vertical motion in an atmosphere, the equation of motion (2.14) and the continuity equation (2.16) become

$$\begin{aligned} \frac{du}{dt} + \frac{1}{\rho} \frac{\partial p}{\partial x} &= fv, \\ \frac{dv}{dt} + \frac{1}{\rho} \frac{\partial p}{\partial y} &= -fu, \\ \frac{\partial u}{\partial x} + \frac{\partial v}{\partial y} &= 0. \end{aligned} \quad (2.17)$$

where $f = 2\Omega \sin\phi$. Operating on the first equation in (2.17) with $\frac{\partial}{\partial y}$ and the second with $\frac{\partial}{\partial x}$ and then subtracting

$$\frac{d}{dt} \left(\frac{\partial v}{\partial x} - \frac{\partial u}{\partial y} \right) + f \left(\frac{\partial v}{\partial y} + \frac{\partial u}{\partial x} \right) + v \frac{\partial f}{\partial y} = 0. \quad (2.18)$$

The second term in (2.18) is zero by the third equation in (2.17). As a further simplification, we may expand the Coriolis parameter f in a Taylor series about the latitude ϕ_o as

$$f = f_o + \beta y + (\text{higher - order terms})$$

where $y = 0$ at ϕ_o , $f_o = 2\Omega \sin\phi_o$ and

$$\beta = \left. \frac{df}{dy} \right|_{\phi_o} = 2\Omega \cos\phi \left. \frac{d\phi}{dy} \right|_{\phi_o} = 2\Omega \left(\cos\phi \frac{1}{\sqrt{1 - \left(\frac{y}{a}\right)^2}} \right)_{\phi_o} = 2\Omega \frac{\cos\phi_o}{a}$$

since $\sin\phi = \frac{y}{a}$. Note that

$$\frac{d}{dt} = \frac{\partial}{\partial t} + u \frac{\partial}{\partial x} + v \frac{\partial}{\partial y}$$

and assume a linear relation between f and y , i.e. we let $f = f_o + \beta y$, equation (2.18) becomes

$$\left(\frac{\partial}{\partial t} + \bar{u} \frac{\partial}{\partial x} \right) \left(\frac{\partial v'}{\partial x} - \frac{\partial u'}{\partial y} \right) + \beta v' = 0. \quad (2.19)$$

If we define a perturbation stream function ψ according to

$$u' = -\frac{\partial\psi}{\partial y}, \quad v' = \frac{\partial\psi}{\partial x},$$

the perturbation form (2.19) then is

$$\left(\frac{\partial}{\partial t} + \bar{u} \frac{\partial}{\partial x} \right) \nabla^2 \psi + \beta \frac{\partial\psi}{\partial x} = 0. \quad (2.20)$$

Assuming a solution exists of the form

$$\psi = \text{Re}\{Ae^{j(\omega t + kx + ly)}\} \quad (2.21)$$

where k and l are wave numbers in the zonal and meridional directions, respectively, substituting from (2.21) into (2.20) gives

$$(\omega + k\bar{u})(-k^2 - l^2) + k\beta = 0,$$

or

$$-\omega = k\bar{u} - \frac{\beta k}{(k^2 + l^2)}. \quad (2.22)$$

Thus for wave solutions (2.21) to be possible the dispersion relation

$$c = -\frac{\omega}{k} = \bar{u} - \frac{\beta}{(k^2 + l^2)} \quad (2.23)$$

must be satisfied. The velocity relative to the zonal flow is $c - \bar{u}$ where c is the phase velocity towards. Rossby waves (planetary waves in their simplest form), therefore, drift to the west relative to the mean flow.

Chapter 3

SIGNAL PROCESSING BACKGROUND

Digital signal processing has a broad spectrum of topics. In this chapter, the emphasis is placed only on spectral estimation (Lim & Oppenheim 1988, p. 58-118) and modeling of data (Press et al. 1989, p. 521 -528) since, in the following chapter, an effort has been made to investigate power spectra of waves with different periods and to model the perturbation of the atmosphere density by the superposition of several sinusoids.

3.1 Spectral Estimation

In digital signal processing, the required spectral estimation is to be generated from a finite set of time series observations. Spectral estimators may be classified as either nonparametric or parametric. Periodogram and Blackman-Tukey are nonparametric estimators while Maximum entropy is a parametric estimator. The nonparametric estimators require no assumptions about the data other than wide-sense stationarity. However, they have the disadvantage that, if the estimator yields good estimates on the average (low bias), then we can expect much variability from one data realization to the next (high variance); if we choose an estimator with low variability, then on the average the spectral estimate may be poor. The only way out of this dilemma is to increase the data record length. The parametric ones, on the other hand, are based on rational transfer function or time series models of the data. Hence, their application is more restrictive. The advantage of the parametric spectral estimator is that when applicable it yields a more accurate spectral esti-

mate. Without having to increase the data record length, we can simultaneously reduce the bias and the variance over the nonparametric estimator. Of course, the improvement is due to the use of *a priori* knowledge afforded by the modeling assumption.

3.1.1 Periodogram and Blackman-Tukey Spectral Estimators

Assuming $x(n)$ is a real discrete-time random process that is wide sense stationary, the power spectral density (PSD) of $x(n)$ is defined as

$$P_x(\omega) = \lim_{M \rightarrow \infty} E \left[\frac{1}{2M+1} \left| \sum_{n=-M}^M x(n) e^{-j\omega n} \right|^2 \right]. \quad (3.1)$$

Equation (3.1) says that the PSD at frequency ω is found by first taking the magnitude squared of the Fourier transform of $x(n)$ and then dividing by the data record length to yield power. Since the power will be a random variable, the expected value is taken.

Corresponding to (3.1), the periodogram spectral estimator is defined as

$$\hat{P}_{PER}(\omega) = \frac{1}{N} \left| \sum_{n=0}^{N-1} x(n) e^{-j\omega n} \right|^2. \quad (3.2)$$

It might be supposed that if enough data were available, say $N \rightarrow \infty$, then

$$\hat{P}_{PER}(\omega) \rightarrow P_x(\omega).$$

This is the case for estimation of the mean. However, the random fluctuation or variance of the periodogram does not decrease with increasing N and hence the periodogram is not a consistent estimator.

Another estimator called Blackman-Tukey is thus developed in the hope that a better estimation can be obtained. The following expression of PSD is considered

to be equivalent to (3.1):

$$P_x(\omega) = \sum_{k=-\infty}^{\infty} r_x(k)e^{-j\omega k}, \quad (3.3)$$

where

$$r_x(k) = E[x(n)x(n+k)] \quad (3.4).$$

the so called periodogram estimator could be expressed as

$$\hat{P}_{PER}(\omega) = \sum_{k=-(n-1)}^{n-1} \hat{r}_x(k)e^{-j\omega k}, \quad (3.5)$$

where

$$\hat{r}_x(k) = \frac{1}{N} \sum_{n=0}^{N-1-|k|} x(n)x(n+|k|) \quad (3.6).$$

Here $\hat{r}_x(k)$ is a biased estimator of the autocorrelation function. The poor performance of the periodogram, that it is not a consistent estimator since the variance does not decrease with increasing data record length, may be attributed to the poor performance of the autocorrelation function estimator. In fact, from equation (3.6), $\hat{r}_x(N-1)$ is estimated by $\frac{1}{N}x(0)x(N-1)$ no matter how large N is. This estimator will be highly variable because of the lack of averaging of lag products, and it will be biased as well. The higher lags of the autocorrelation function will be poorer estimates since they involve fewer lag products.

One way to avoid this problem is to weight the higher lags less, which gives rise to Blackman-Tukey spectral estimator

$$\hat{P}_{BT}(\omega) = \sum_{k=-(N-1)}^{N-1} w(k)\hat{r}_x(k)e^{-j\omega k}, \quad (3.7)$$

where $w(k)$ is a weight function, called the *lag window*. If the Bartlett window is selected, then

$$w(k) = \begin{cases} 1 - \frac{|k|}{M}, & \text{if } |k| \leq M \\ 0, & \text{if } |k| > M \end{cases}. \quad (3.8)$$

The Blackman-Tukey estimator (3.7) has the advantage that the variance can be suppressed. However, this is obtained at the cost of increased bias in the mean. Much of the art in nonparametric spectral estimation, therefore, is in choosing an appropriate window, both in type and in length.

3.1.2 Maximum Entropy Estimator

Maximum entropy spectral estimation is based on an explicit extrapolation of a segment of a known autocorrelation function for the samples that are not known. Suppose $\{r(0), r(1), \dots, r(p)\}$ is known, then the question arises as to how $\{r(p+1), r(p+2), \dots\}$ should be specified in order to guarantee that the entire autocorrelation function is valid or that its Fourier transform is nonnegative. In general, there are an infinite number of possible extrapolations, all of which yield valid autocorrelation functions. In the maximum entropy method, it is argued that the time series characterized by the extrapolated autocorrelation function has maximum entropy. The time series will then be the most random one.

The word *entropy* arises from the measurement of information. Assume that p is the probability of occurrence of a message and I is the information gained from the message. We know that a message that is certain to happen (having a probability of unity) conveys no information while a message that is almost impossible to happen (having a probability of zero) conveys a large amount of information. Hence when $p \rightarrow 1, I \rightarrow 0$ and when $p \rightarrow 0, I \rightarrow 1$. This suggests the following

$$I \sim \log \frac{1}{p}.$$

Suppose that we have a communication system which transmits M different messages $\{m_1, m_2, \dots\}$, with probabilities of occurrence denoted by $\{p_1, p_2, \dots\}$, respec-

tively. Suppose further that during a long period of transmission, a sequence of L messages has been generated. If L is large, then, on the average, we may expect to find in the sequence $p_1 L$ messages of m_1 , $p_2 L$ messages of m_2 and so on. The total information in such a sequence is given by (Lathi 1983, p. 608-612)

$$I_{total} = (p_1 L) \log_2 \left(\frac{1}{p_1} \right) + (p_2 L) \log_2 \left(\frac{1}{p_2} \right) + \dots$$

The average information per message interval, represented by the symbol H , is therefore

$$H = \frac{I_{total}}{L} = \sum_{k=1}^M p_k \log_2 \left(\frac{1}{p_k} \right).$$

The quantity H is the entropy.

If we consider a time series $\{x(n)\}$ that is Gaussian distributed and limited to the frequency band $-f_B \leq f_o \leq f_B$, then the entropy per sample at the Nyquist rate has the form (Haykin 1979, p. 16-70)

$$E \propto \int_{-\frac{1}{2}}^{\frac{1}{2}} \ln P(f) df, \quad (3.9)$$

where $f = f_o/f_s$ in which f_s is the sampling frequency and $P(f)$ is the PSD of the process $x(n)$. From (3.3), the PSD of $x(n)$ is

$$P(f) = \sum_{k=-\infty}^{\infty} r(k) e^{-j2\pi f k}. \quad (3.10)$$

The autocorrelation function is obtained by taking the inverse Fourier transformation, i.e.

$$r(k) = \int_{-\frac{1}{2}}^{\frac{1}{2}} P(f) e^{j2\pi f k} df. \quad (3.11)$$

Our interest here is to find the spectral density estimate $\hat{P}(f)$ provided $\{r(0), r(1), \dots, r(p)\}$ is known and $\{r(p+1), r(p+2), \dots\}$ has maximum entropy. We

therefore differentiate the entropy E in (3.9) with respect to $r(n)$, where $|n| > p$, and set the result to be zero to get

$$\int_{-\frac{1}{2}}^{\frac{1}{2}} \frac{\partial \ln \hat{P}(f)}{\partial r(n)} df = \int_{-\frac{1}{2}}^{\frac{1}{2}} \frac{1}{\hat{P}(f)} \frac{\partial \hat{P}(f)}{\partial r(n)} df = 0, \quad |n| > p. \quad (3.12)$$

Using (3.10) and noting that n is arbitrary but fixed, equation (3.12) becomes

$$\int_{-\frac{1}{2}}^{\frac{1}{2}} \frac{\partial \ln \hat{P}(f)}{\partial r(n)} df = \int_{-\frac{1}{2}}^{\frac{1}{2}} \frac{1}{\hat{P}(f)} e^{-j2\pi fn} df = 0, \quad |n| > p. \quad (3.13)$$

Expanding $\frac{1}{\hat{P}(f)}$ in Fourier series,

$$\frac{1}{\hat{P}(f)} = \sum_{n=-\infty}^{\infty} c_n e^{-j2\pi fn}, \quad -\frac{1}{2} \leq f \leq \frac{1}{2}, \quad (3.14)$$

where c_n can be determined as

$$c_n = \begin{cases} \int_{-\frac{1}{2}}^{\frac{1}{2}} \frac{1}{\hat{P}(f)} e^{j2\pi fn} df, & |n| \leq p \\ = 0, & |n| > p \end{cases} \quad (3.15)$$

That $c_n = 0$ if $|n| > p$ is obtained by taking the complex conjugate of the left-hand side of (3.13). From (3.14), the estimate of PSD may be expressed as

$$\hat{P}(f) = \frac{1}{\sum_{n=-p}^p c_n e^{-j2\pi fn}} \quad (3.16)$$

Equation (3.16) is equivalent to the following form (Haykin 1979, p. 18-20)

$$P(f) = \frac{\sigma^2}{|1 + \sum_{k=1}^p a(k) e^{-j2\pi fk}|^2}. \quad (3.17)$$

Equation (3.17) happens to take on an identical form to the autoregressive (AR) model, which is another parametric spectral estimator. In other words, the principle of maximum entropy and the representation of the process $x(n)$ by an autoregressive model are equivalent. The coefficients $\{a(1), a(2), \dots, a(p), \sigma^2\}$ in (3.17) can be found by solving the celebrated Yule-Walker equations using the known samples, $\{r(0), r(1), \dots, r(p)\}$, of the autocorrelation functions (Bose 1985, p. 361-372).

3.2 Modeling of Data

An assumption is made that the long term density perturbations of the atmosphere can be modeled by the superposition of several sinusoids with specific periods, namely

$$D(x, t) = \text{Re} \left\{ \sum_i A_i e^{j(\omega_i t - kx)} \right\} = \text{Re} \left\{ \sum_i (c_i + jd_i) e^{j(\omega_i t - kx)} \right\}, \quad (3.18)$$

where D is the density ratio of the atmosphere, x is the horizontal spatial coordinate, t is time, $A_i = c_i + jd_i$ is the complex amplitude and k is the wave number in the x direction. Taking ω_i (frequency), $(c_i^2 + d_i^2)^{\frac{1}{2}}$ (amplitude) and $\tan^{-1} \frac{d_i}{c_i}$ (phase angle) to be the parameters of the model, we now consider fitting when the model depends nonlinearly on the set of M unknown parameters $a_k, k = 1, 2, \dots, M$, denoted by \vec{a} . For simplicity, x is fixed so that D is the function of t and \vec{a} only. The model to be fitted becomes

$$D = D(t; \vec{a}). \quad (3.19)$$

A merit function χ is defined as

$$\chi(\vec{a}) = \sum_{i=1}^N \left[\frac{D_i - D(t_i; \vec{a})}{\sigma_i} \right]^2, \quad (3.20)$$

where \vec{a} is the parameter array and σ_i is the variance for each signal, and the best-fit parameters will be determined by its minimization. If the current approximation $D(t_i; \vec{a}_{cur})$ is a good one, we jump from the current trial parameters \vec{a}_{cur} to the minimizing ones \vec{a}_{min} , namely

$$\vec{a}_{min} = \vec{a}_{cur} + \mathbf{C}^{-1} \cdot [-\nabla \chi(\vec{a}_{cur})], \quad (3.21)$$

where \mathbf{C} is the matrix whose components are the second partial derivatives of the merit function. If $D(t_i; \vec{a}_{cur})$ is a poor one, we try to take a step down the gradient

$\nabla\chi$. Thus

$$\vec{a}_{next} = \vec{a}_{cur} - constant \cdot \nabla\chi(\vec{a}_{cur}), \quad (3.22)$$

where the constant is small enough not to exhaust the downhill direction.

The gradient of χ with respect to \vec{a} has components

$$\frac{\partial\chi}{\partial a_k} = -2 \sum_{i=1}^N \frac{[D_i - D(t_i; \vec{a})]}{\sigma_i^2} \frac{\partial D(x; \vec{a})}{\partial a_k}, \quad (3.23)$$

and the matrix C in (3.21) is obtained by taking the second partial derivative of χ , namely

$$\frac{\partial^2\chi}{\partial a_k \partial a_l} = 2 \sum_{i=1}^N \frac{1}{\sigma_i^2} \left[\frac{\partial D(t_i; \vec{a})}{\partial a_k} \frac{\partial D(t_i; \vec{a})}{\partial a_l} - [D_i - D(t_i; \vec{a})] \frac{\partial^2 D(t_i; \vec{a})}{\partial a_k \partial a_l} \right]. \quad (3.24)$$

The second derivative term $\frac{\partial^2 D}{\partial a_k \partial a_l}$ can be ignored here because $D_i - D(t_i; \vec{a})$ is small. Further more, if we let

$$\beta_k = -\frac{1}{2} \frac{\partial\chi}{\partial a_k} \quad (3.25)$$

and

$$\alpha_{kl} = \frac{1}{2} \frac{\partial^2\chi}{\partial a_k \partial a_l}, \quad (3.26)$$

by making $[\alpha] = \frac{1}{2}C$, (3.21) can be rewritten as the set of linear equations

$$\sum_{l=1}^M \alpha_{kl} \delta a_l = \beta_k. \quad (3.27)$$

where $\delta\vec{a} = \vec{a}_{cur} - \vec{a}_{min}$. Likewise, (3.22) becomes

$$\delta a_l = constant \cdot \beta_l. \quad (3.28)$$

Since the model (3.18) depends nonlinearly on the parameter array \vec{a} , the minimization of χ proceeds iteratively. Given trial values for the parameters, the above procedure is repeated to improve the trial solution until χ stops decreasing.

Chapter 4

CHARACTERISTICS OF ATMOSPHERIC WAVES DURING STRATOSPHERIC WARMING PERIODS

In this chapter, the characteristics of planetary waves and gravity waves during the stratospheric warming that was observed in February-March 1986 are reported. First, a one-dimensional planetary wave model was developed with the help of power spectral estimation as well as nonlinear fitting. The agreement of the modeled atmospheric densities and the measured ones showed that the density perturbation in the atmosphere can be approximated by the superposition of only a few sinusoids. Then a spatial power spectral estimation was applied to the signals with short periods in the hope of revealing the characteristics of gravity waves during the stratospheric warming. The result shows that the warming period corresponds to a periodic enhancement of wave activity in the stratosphere and the weakening of gravity wave activity in the mesosphere, which could be caused by the descending of the level of significant wave breaking due to the constructive interference of the planetary waves.

4.1 Characteristics of the Planetary Waves

To find the periods, phase shifts and the amplitudes of the planetary waves, a one-dimensional model was developed to simulate the density variation between February 15 and March 9, 1986. The model has the following form:

$$D(x, t) = \text{Re} \left\{ \sum_i A_i e^{j(\omega_i t - kx)} \right\} = \text{Re} \left\{ \sum_i (c_i + j d_i) e^{j(\omega_i t - kx)} \right\}, \quad (4.1)$$

where D is the density ratio of the atmosphere, x is the horizontal spatial coordinate, t is time, $A_i = c_i + jd_i$ is the complex amplitude and k is the wave number in x direction.

Since the measurement was done at a fixed place, x can be, without loss of generality, set to be zero in the above model. Now that only the time development of the waves needs to be simulated, the parameters to be estimated are as follows:

$$\begin{aligned}
 \omega_i &: \text{frequency} \\
 (c_i^2 + d_i^2)^{\frac{1}{2}} &: \text{amplitude} \\
 \tan^{-1} \frac{d_i}{c_i} &: \text{phase}
 \end{aligned} \tag{4.2}$$

The frequencies of the planetary waves were determined by power spectral estimation. In Chapter 3 we realized that the estimation of the power density will be more reliable if the measured data record is sufficiently long. Unfortunately, where there were only 22 full-night mean densities available. To achieve a better spectral estimation, both parametric and nonparametric estimators were used and the results were compared.

For convenience, the densities had been converted to density ratios by using the U. S. Standard Atmosphere 1976 as the basis. The mean of the densities at each altitude (5 km steps, from 25 km to 65 km) had been subtracted so that the expectation of the signals became zero. The power density spectral estimators, both parametric and nonparametric, were then used to explore the power spectra at the different altitudes.

Figure 5(a) shows the results from the Blackman-Tukey estimator. One can see that even though the signal had zero mean, the DC components in the power spectra were not zero. This is because once a Bartlett window (3.8) had been used,

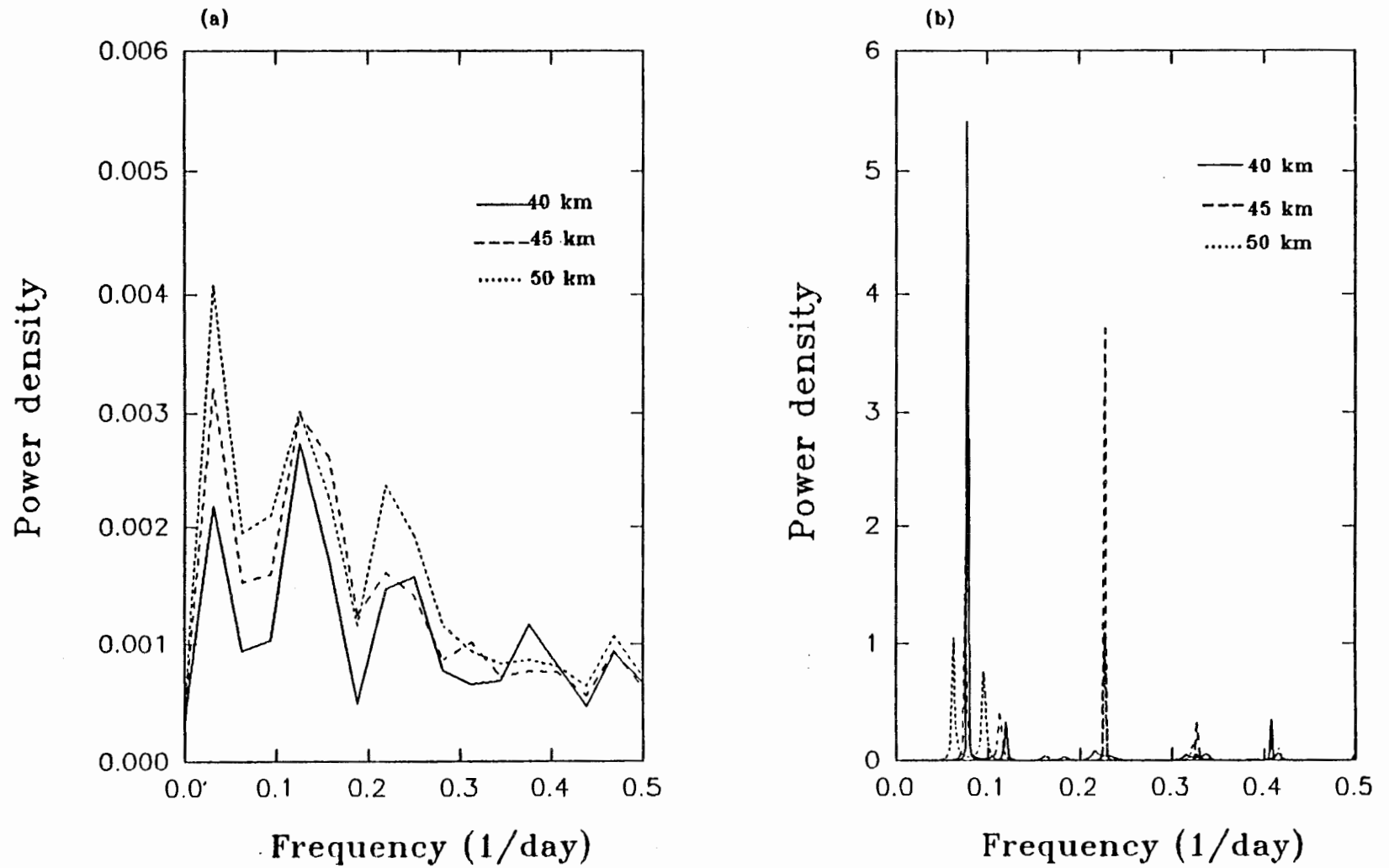


Fig. 5. Comparison of the results of the two spectral estimators.
(a) Blackman-Tukey. (b) Maximum Entropy.

the autocorrelation lag estimate became

$$\hat{r}_{eq}(k) = \left(1 - \frac{|k|}{M}\right) \hat{r}_x(k) \quad (4.3)$$

which represented a biased estimate. Likewise, this estimator tended to give some low frequency components which were not present in the results of Maximum Entropy estimator (Figure 5(b)). Figure 6 shows the estimated power spectra at all altitudes (from 25 km to 65 km, 5 km steps) by the Maximum Entropy method. Since the purpose was to find that at which frequencies most of the signal power resided, a high order ($M = 15$) estimator was used, which could pick the most dominant frequencies. It is interesting to see that the power of the signal resided at some particular frequencies, such as $f_1 = 0.07$, $f_2 = 0.10$, $f_3 = 0.225$ and $f_4 = 0.33$. Thus the frequencies ω_i in the model could be easily determined. The number of the frequencies being selected also implies the number of sinusoids embedded in the density signal.

A computer program was developed to perform the nonlinear fitting. With frequencies being fixed, amplitudes and phases of the four waves were represented by a parameter array \vec{a} . A merit function was defined which depended on the known density signal as well as the unknown parameter array \vec{a} (see Chapter 3, equation (3.20)). The array \vec{a} was updated by the minimization of the merit function. Since the model was dependent nonlinearly on the parameters, the minimization was carried out iteratively after trial values were given.

The result of the simulation is shown in Figure 7. The comparison of the modeled density perturbations and the measured ones is presented in Figure 8. The satisfactory agreement in turn gives credibility to the Maximum Entropy method used in the power spectral estimation.

From the model, the phase shifts of the principal wave components versus

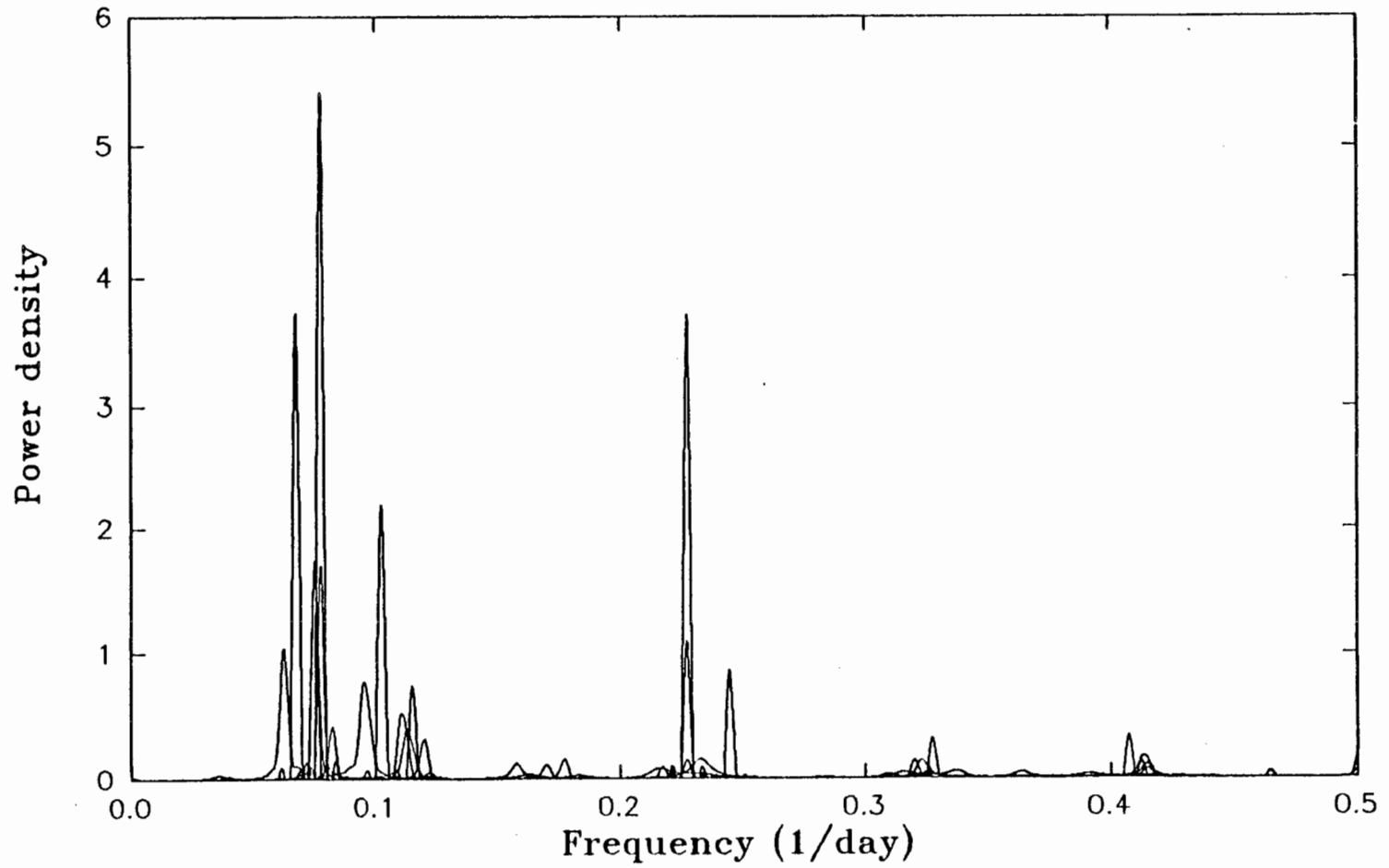


Fig. 6 Spectral estimation by MEM at all altitudes

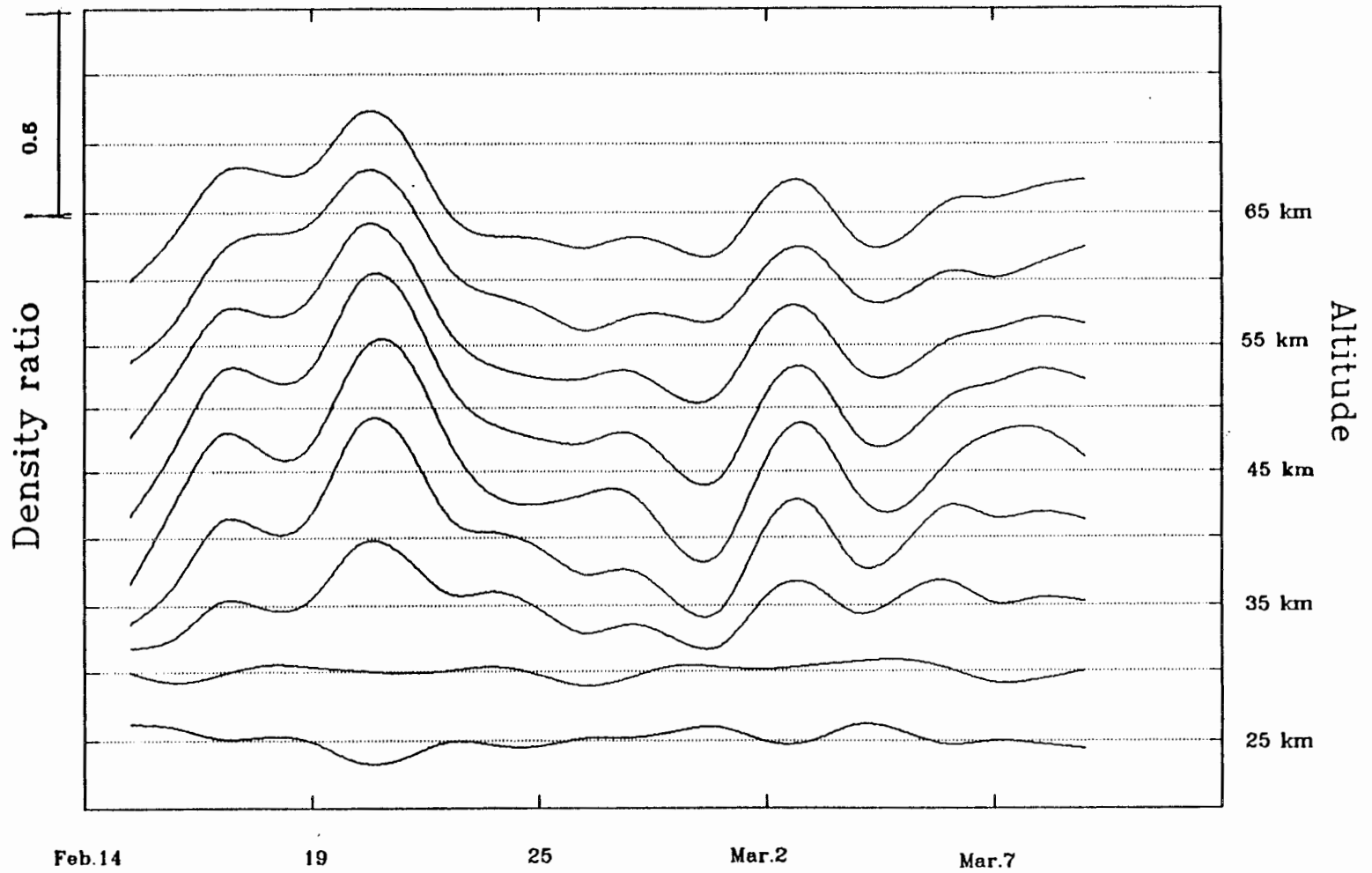


Fig. 7. Modeled density variations

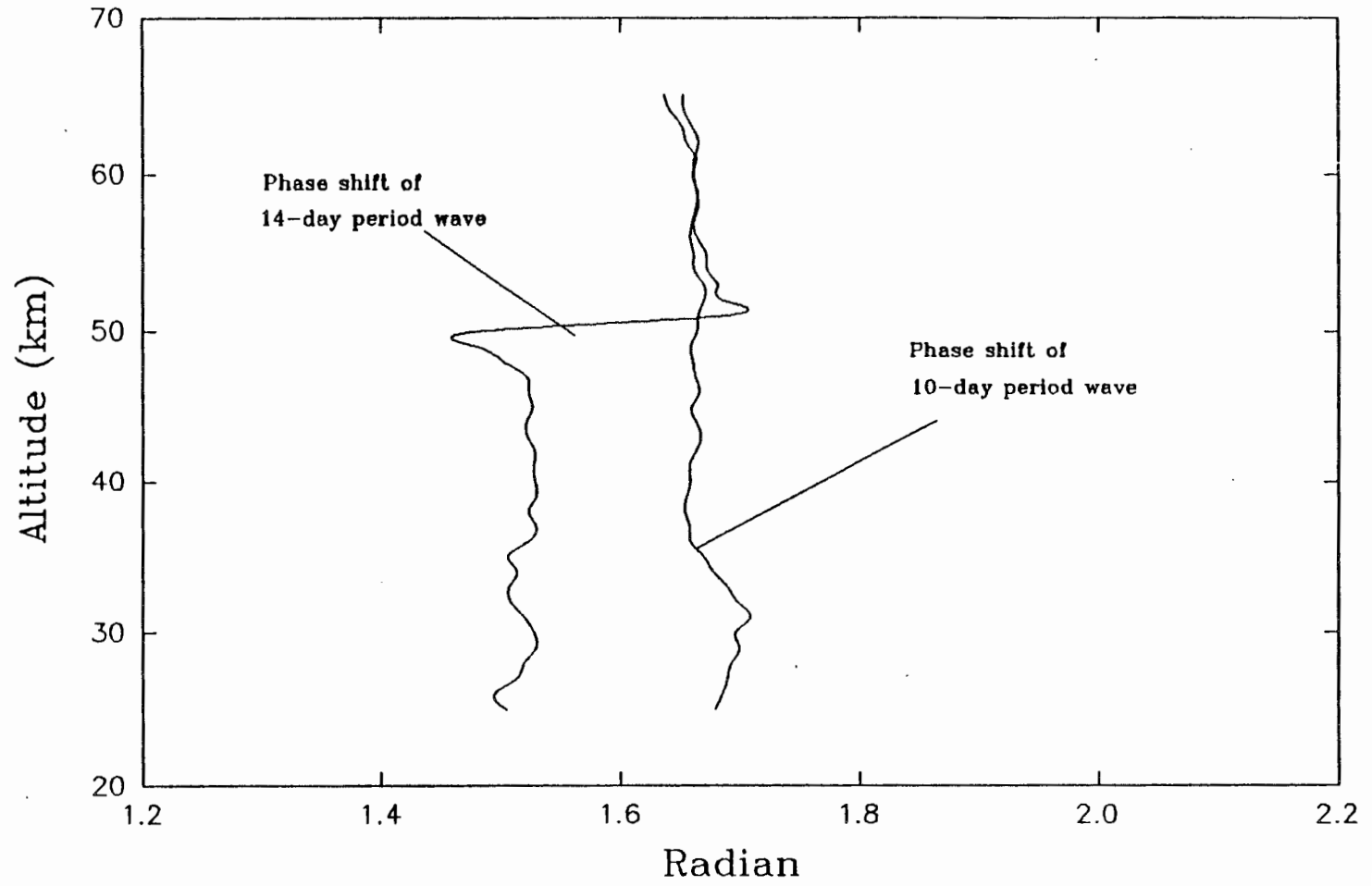
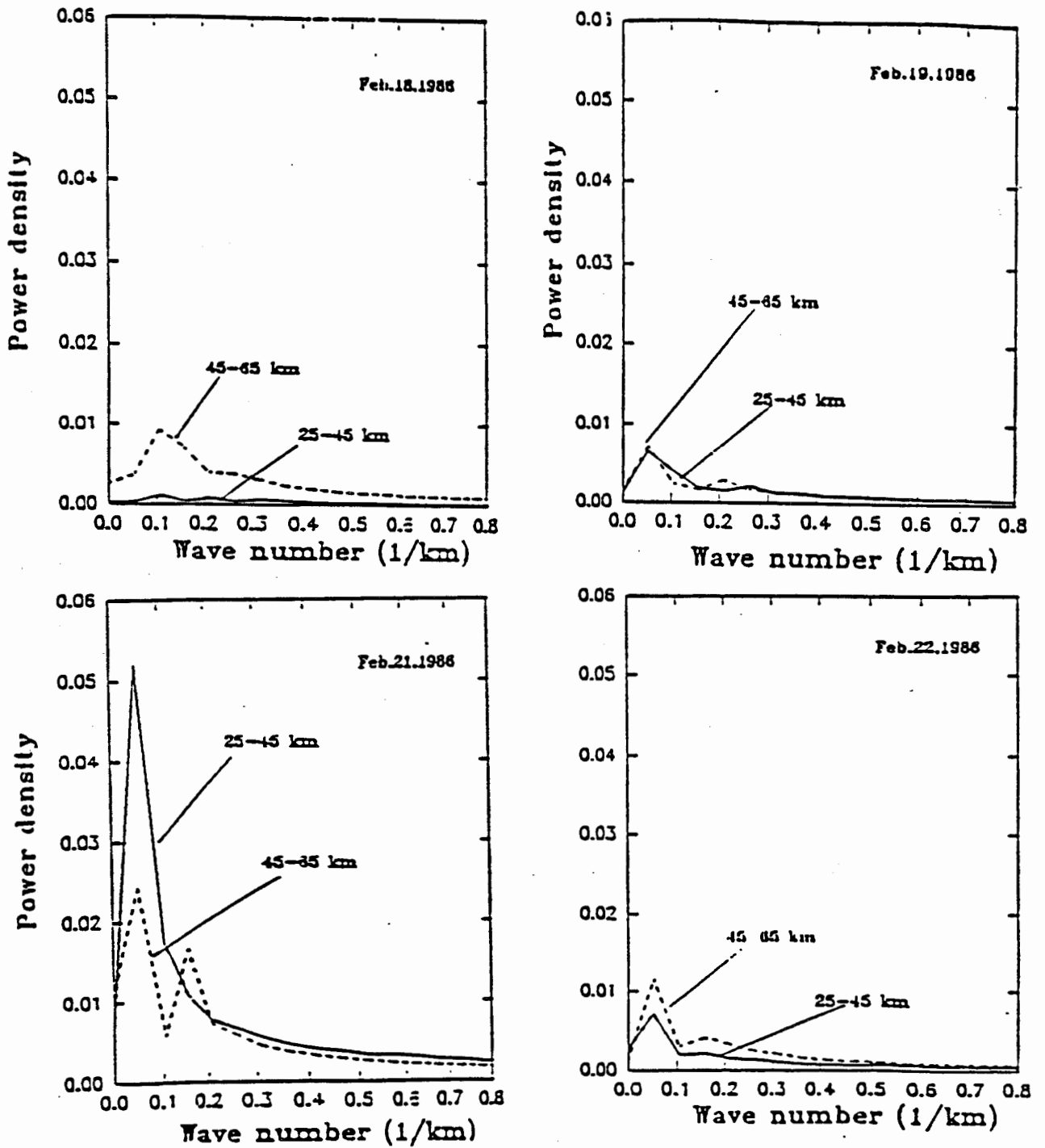
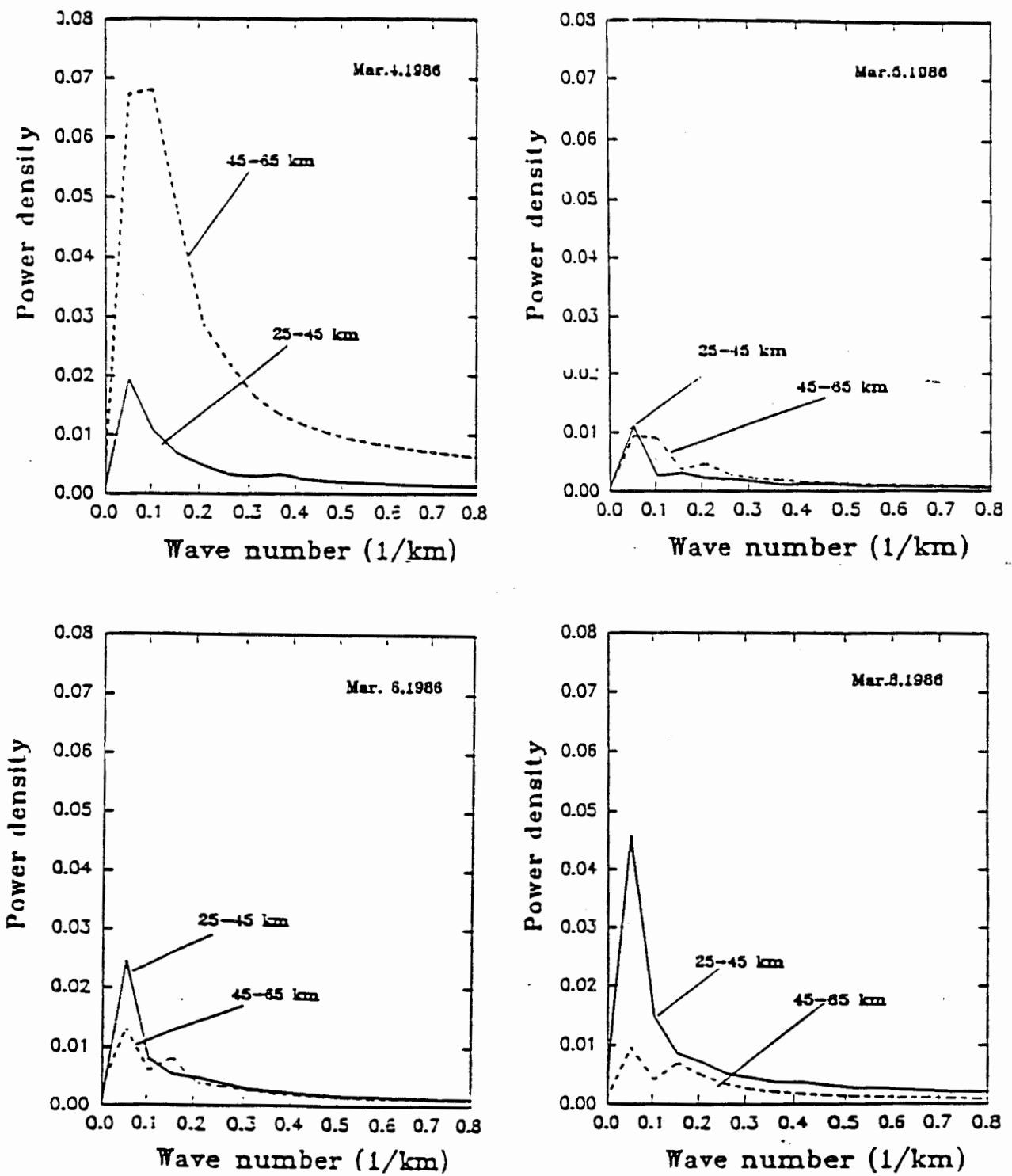


Fig. 9 Phase shift of the two principle wave components



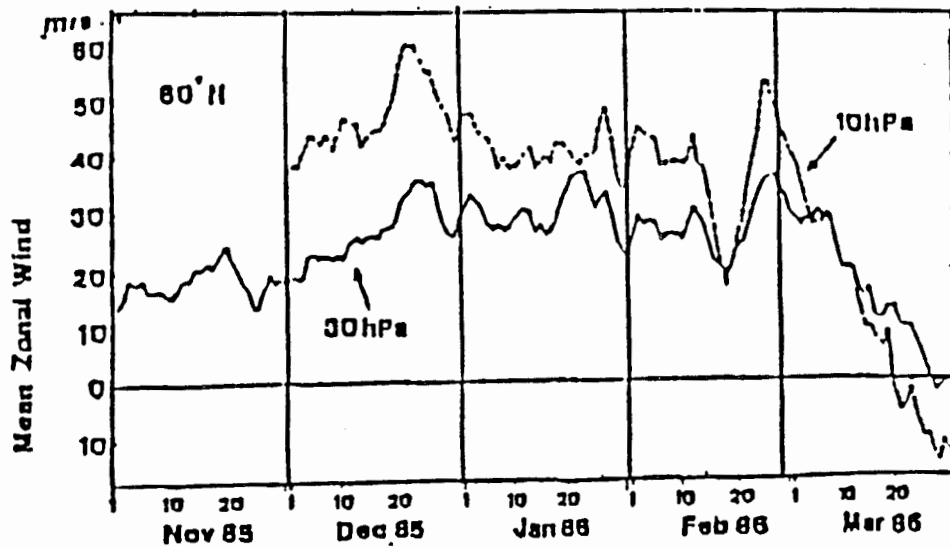
(a) February 18-22.

Fig. 10. Gravity wave spectra at different altitude ranges around stratospheric warming periods. (Figure continues.)

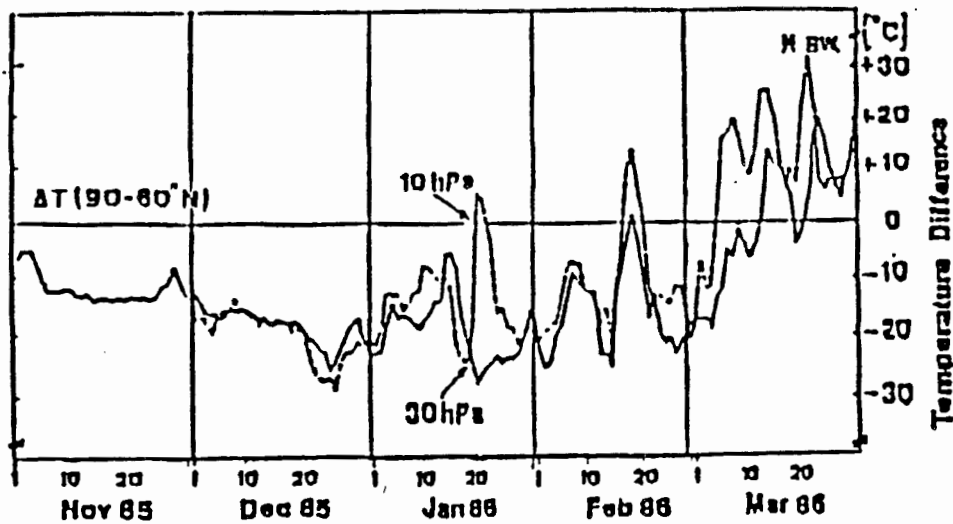


(b) March 4-8.

Fig. 10. Continued.



(a) Mean zonal wind (m/s) at $60^{\circ}N$, 10 and 30 hpa.



(b) Temperature difference ($^{\circ}C$) between $60^{\circ}N$ and the pole, 10 and 30 hpa.

Fig. 11. Mean zonal wind and temperature differences in the winter of 1986 based on satellite data. (From Naujokat and Labitzke, 1986)

Since the amplitudes of gravity waves tend to grow exponentially while the waves are propagating upward. Thus we expected to see greater magnitudes of the power spectra at 45-65 km range than that at 25-45 km. However, Figure 10 shows the contrary during the stratospheric warming periods. The weakened gravity wave activity at 45-65 km could be explained as the constructive interference of the planetary waves modulating the stability of the surrounding atmosphere at about 50 km, so that the level of significant wave breaking was lowered to that altitude. Such phenomena had been discussed by Lindzen (1981) and Fritts (1984).

Chapter 5

CONCLUSIONS

Middle atmosphere densities measured by a Rayleigh scatter lidar during February and March 1986 showed strong wave-like perturbations. The high resolution sequences of the continuous measurements provided a solid base for the simulation of the long period variations as well as the investigation of the gravity wave activity.

The long-term perturbations of the density were modeled satisfactorily with a superposition of several sinusoids. Periods of the sinusoids were found to be 14, 10, 4 and 3 days by spectral analysis at the fixed altitudes. If a horizontal velocity of 10 m/s is assumed as typical of synoptic scales, the first two sinusoids with the periods of 10 and 14 days correspond to planetary wave 1 and 2.

The spatial spectrum analysis of the gravity waves showed strong wave activity at 25-45 km during stratospheric warming periods. The weakening of gravity wave activity at 45-65 km during the warming periods implied that the level of significant wave breaking was lowered to below 50 km during the event, which could be explained as the constructive interference of the planetary waves had modulated the stability of the surrounding atmosphere.

While the source for the stratospheric warming must be from the large energy source of the planetary waves, the mechanism for the event is not clear. It may be that the constructive interference of the planetary waves results in such large density perturbations that the stability of the stratosphere is upset. In fact, planetary wave breaking could be the physical process that leads to the large amount of small scale wave structure observed near the peak of the event (the large vorticity increase). The planetary wave breaking would generate a range of scales of shorter waves and

vortices as the atmosphere re-establishes equilibrium. The observed temperature increase, for which these events are named, may be just the normal response of the adiabatic heating of the higher density at about two scale heights above, due to the constructive interference of the waves.

REFERENCES

- D. G. Andrews, J. R. Holton, and C. B. Leovy, *Middle atmosphere dynamics*. New York: Academic Press, 1987.
- N. K. Bose, *Digital filter*. New York: Elsevier Science Publishing Company, 1985.
- D. C. Fritts, "Gravity waves saturation in the middle atmosphere: A review of theory and observation," *Rev. Geophys.*, vol. 22, pp. 275-307, 1984.
- S. Haykin, "Nonlinear methods of spectral analysis," in *Topics in Appl. Phys.*, vol. 34. New York: Springer-Verlag, Berlin and Heidelberg, 1979.
- P. H. Haynes and M. E. McIntyre, "On the representation of Rossby-wave critical layers and wave breaking in zonally truncated models," *J. Atmos. Sci.*, vol. 44, pp. 2359-2382, 1986.
- J. R. Holton, *An introduction to dynamic meteorology*. New York: Academic Press, 1979.
- J. R. Holton, "The influence of gravity wave breaking on the general circulation of the middle atmosphere," *J. Atmos. Sci.*, vol. 39, pp. 791-799, 1982.
- J. T. Houghton, *The physics of atmosphere*. London: Cambridge University Press, 1986.
- B. P. Lathi, *Modern digital and analog communication systems*. New York: Holt, Rinehart, and Winston, 1983.
- J. S. Lim and A. V. Oppenheim, *Advanced topics in signal processing*. Englewood Cliffs, New Jersey: Prentice Hall, 1988.

- R. S. Lindzen, "Turbulence and stress owing to gravity wave and tide breakdown," *J. Geophys. Res.*, vol. 86, pp. 9707-9714, 1981.
- M. E. McIntyre and T. M. Palmer, "Breaking planetary waves in the stratosphere," *Nature*, vol. 305, pp. 593-600, 1983.
- B. Naujokat and K. Labitzke, "Beilage zur berliner wetterkarte," *Climate Analysis CTR*, 1986.
- D. Offermann, R. Gerndt, R. Kuchler, K. Baker, W. R. Pendleton, W. Meyer, U. von Zahn, C. R. Philbrick, and F. J. Schmidlin, "Mean state and long term variations of temperature in the winter middle atmosphere above northern Scandinavia," *J. Atmos. & Terres. Phys.*, vol. 49, pp. 655-674, 1987.
- C. R. Philbrick, F. J. Schmidlin, K. U. Grossman, G. Lange, D. Offerman, K. D. Baker, D. Krankowsky, and U. von Zahn, "Density and temperature structure over northern Europe," *J. Atmos. Terr. Phys.*, vol. 47, pp. 159-172, 1985.
- C. R. Philbrick, D. P. Sipler, G. Davidson, and W. P. Moskowitz, "Remote sensing of structure properties in the middle atmosphere using lidar," *Proceedings of OSA Meeting on Laser and Optical Remote Sensing*, pp. 120-123, 1987.
- C. R. Philbrick, D. P. Sipler, B. E. Dix, G. Davidson, W.P. Moskowitz, C. Trowbridge, R. Sluder, F.J. Schmidlin, L.D. Mendenhall, K.H. Bhavnani, and K.J. Hahn, "Measurements of the high latitude middle atmosphere properties using LIDAR," *AFGL-TR-87-0053*, 1987.
- W. H. Press, B.P. Flannery, S.A. Teukolsky, and W.T. Vetterling, *Numerical recipes*. New York: Cambridge University Press, 1989.
- M. L. Salby, "Survey of planetary-scale traveling waves: The state of theory and observations," *Revs. Geophys. Space Phys.*, vol. 22, pp. 209-236, 1984.

Appendix
COMPUTER PROGRAMS

1. FIT.FOR—Program to perform nonlinear fitting of data.
2. MEM.FOR—Program to perform spectral estimation with Maximum Entropy estimator.
3. PICK5.FOR—Program to lift the data needed from profiles.
4. GSP.FOR—Program to extract gravity wave signals from profiles.
5. PDM.FOR—Program to perform spacial spectral estimation with Blackman-Tukey estimator.

PROGRAM FIT

```

C THIS PROGRAM IS USED TO FIT THE GIVEN DATA TO A NONLINEAR
C MODEL, NAMELY, A SUPERPOSITION OF 4 SINUSOIDS. THE
C FREQUENCIES OF THE SINUSOIDS HAVE BEEN ALREADY DETERMINED BY
C MAXIMUM ENTROPY METHOD. THE AMPLITUDES AND THE PHASES ARE TO
C BE FITTED ITERATIVELY IN THIS PROGRAM.
C INPUT OF THIS PROGRAM:
C DA4.DAT. THIS IS A DATA FILE CONTAINING EQUAL SPACED DENSITIES
C AT DIFFERENT ALTITUDES (5 KM STEPS, FROM 25 TO 65 KM) FROM
C FEB.15 TO MAR.9,1986 (CERTAIN INTERPOLATION HAS BEEN DONE).
C OUTPUT OF THIS PROGRAM:
C 1. A0.DAT,...,I0.DAT. THOSE ARE MODELED DENSITIES AT DIFFERENT
C ALTITUDES (5 KM STEPS, 9 LEVELS).
C 2. SINUSOID.DAT. THIS IS A FORMATED FILE CONTAINING THE TABLE OF
C THE AMPLITUDES, PHASES AND PERIODS OF THE SINUSOIDS.
C 3. ERROR.DAT. THIS IS THE FILE CONTAINING THE SQUARED ERROR
C BETWEEN THE MODELED AND THE MEASURED DENSITIES.

DIMENSION X(30),Y(30),YDAT(30,30),SIG(30),A(20),LISTA(20),
* COVAR(20,20),ALPHA(20,20),ERROR(15)
CHARACTER CHAR1*1,CHAR2*2,CHAR3*2
DATA X/1.,2.,3.,4.,5.,6.,7.,8.,9.,10.,11.,12.,13.,14.,15.,16.,
* 17.,18.,19.,20.,21.,22.,23.,24.,25.,26.,27.,28.,29.,30./
DATA SIG/30*1./
DATA LISTA/1,3,4,6,7,9,10,12,12*0/
C TRY TO MODEL THE DENSITY DISTRIBUTION BY THE SUM OF THREE
C HARMONIC WAVES WITH PERIODS 16,12,10 AND 4 DAYS,RESPECTIVELY.

C PRINT *, 'ENTER THE TOTAL NUMBER OF PARAMETERS OF THE MODEL, MA.
C * NOTE THAT MA<=20.'
C READ *, MA
C PRINT*, 'ENTER THE NUMBER OF THE PARAMETERS TO BE ADJUSTED,MFIT.
C * NOTE THAT MFIT<=MA.'
C READ *, MFIT
MA=12
MFIT=8
NCA=MFIT
NDATA=22
LEVL=9
NW=4
TPI=6.2831852
OPEN(UNIT=3,TYPE='OLD',NAME='DA4')
DO I=1,LEVL
DO J=1,NDATA
READ(3,*) YDAT(I,J)
ENDDO
ENDDO
CLOSE(3)
OPEN(UNIT=6,TYPE='NEW',NAME='SINUSOID')
WRITE(6,*) 'SINUSOIDS AT DIFFERENT ALTITUDES:'

```

```

DO 150 I=1,LEVL
DO J=1,NDATA
    Y(J)=YDAT(I,J)
ENDDO
100 DO J=1,MA
    A(J)=1.
ENDDO
C PRINT *, 'ENTER THE FREQUENCY FOR EACH OF THE 4 HARMONICS.'
A(2)=.07
A(5)=.10
A(8)=.225
A(11)=.325
C PRINT *, 'ARE THE PARAMETERS CORRECT ? ENTER Y/N.'
C ACCEPT 5, CHAR2
5 FORMAT(A1)
C IF(CHAR2.EQ.'N'.OR.CHAR2.EQ.'n') THEN
C PRINT *, 'ENTER THE PARAMETERS AGAIN.'
C GOTO 100
C
C ENDIF
ALAMDA=-1.
CHISQ0=1.

CHISQ=0.
DO WHILE(CHISQ.LT.CHISQ0)
    CALL MRQMIN(X,Y,SIG,NDATA,A,MA,LISTA,MFIT,
* COVAR,ALPHA,NCA,CHISQ,CHISQ0,ALAMDA)

ENDDO
PRINT *, 'ERROR=',CHISQ
PRINT *, 'DO YOU WANT TO AJUST THE PARAMETERS OF THE HARMONIC
* WAVES ? ENTER Y/N'
ACCEPT 5,CHAR1
IF(CHAR1.EQ.'Y'.OR.CHAR1.EQ.'y') GOTO 100
ERROR(I)=CHISQ
J1=I+64
CHAR3=CHAR(J1) //'0'
OPEN(UNIT=4,TYPE='NEW',NAME=CHAR3)
DO I1=1,NDATA
    Y1=0.
DO L=1,MA-1,3
    Y1=Y1+A(L)*SIN(TPI*A(L+1)*X(I1)+A(L+2))
ENDDO
WRITE(4,*) X(I1),Y1
ENDDO
CLOSE(4)
C WRITE DOWN THE HARMONIC FUNCTIONS OBTAINED.
WRITE(6,*)
WRITE(6,8) 25+5*(I-1)
8 FORMAT(1H , 'ALTITUDE=' ,I3)
WRITE(6,*)
WRITE(6,10)

```

```

10          FORMAT(1H , '1ST SINOSOID, 2ND SINOSOID, 3RD SINOSOID,
1 4TH SINOSOID' )
          DO L=1,MA/NW
              WRITE(6,20) A(L),A(L+3),A(L+6),A(L+9)
20          FORMAT(4F14.10)
          ENDDO
          WRITE(6,*)
          PRINT*,'THIS LEVEL IS DONE. ENTER PARAMETERS FOR NEXT LEVEL'
150 CONTINUE
          OPEN(UNIT=4,TYPE='NEW',NAME='ERROR')
          DO I=1,LEVL
              WRITE(4,*) I,ERROR(I)
          ENDDO
          CLOSE(4)
          CLOSE(6)
          STOP
          END

          SUBROUTINE MRQMIN(X,Y,SIG,NDATA,A,MA,LISTA,MFIT,
*          COVAR,ALPHA,NCA,CHISQ,CHISQ0,ALAMDA)
C          SET TO LARGEST NUMBER OF FIT PARAMETERS
          PARAMETER (MMAX=20)
          DIMENSION X(NDATA),Y(NDATA),SIG(NDATA),A(MA),LISTA(MA),
*          COVAR(NCA,NCA),ALPHA(NCA,NCA),ATRY(MMAX),BETA(MMAX),DA(MMAX)

          IF(ALAMDA.LT.0) THEN
C          INITIALIZATON
          KK=MFIT+1
          DO 12 J=1,MA
C          DOES LISTA CONTAIN A PROPER PERMUTATION OF THE COEFFICIENTS ?
          IHIT=0
          DO 11 K=1,MFIT
              IF(LISTA(K).EQ.J) IHIT=IHIT+1
11          CONTINUE
          IF(IHIT.EQ.0) THEN
              LISTA(KK)=J
              KK=KK+1
          ELSE IF(IHIT.GT.1) THEN
              PAUSE 'IMPROPER PERMUTATION IN LISTA'
          ENDIF
12          CONTINUE
          IF(KK.NE.(MA+1)) PAUSE 'IMPROPER PERMUTATION IN LISTA'
          ALAMDA=0.001
          CALL MRQCOF(X,Y,SIG,NDATA,A,MA,LISTA,MFIT,ALPHA,BETA,NCA,
*          CHISQ)
          OCHISQ=CHISQ
          DO 13 J=1,MA
              ATRY(J)=A(J)
13          CONTINUE

```

```

ENDIF

C   AFTER LINEARIZED FITTING MATRIX, BY AUGMENTING DIAGONAL ELEMENTS.
DO 15 J=1, MFIT
  DO 14 K=1, MFIT
    COVAR(J,K)=ALPHA(J,K)
14  CONTINUE
    COVAR(J,J)=ALPHA(J,J)*(1.+ALAMDA)
    DA(J)=BETA(J)
15  CONTINUE

C   MATRIX SOLUTION
CALL GAUSSJ(COVAR,MFIT,NCA,DA,1,1)

IF (ALAMDA.EQ.0) THEN
C   ONCE CONVERGED EVALUATE COVARIANCE MATRIX WITH ALAMDA=0.
CALL COVSRT(COVAR,NCA,MA,LISTA,MFIT)
RETURN
ENDIF

DO 16 J=1, MFIT
C   DID THE TRIAL SUCCEED ?
  ATRY(LISTA(J))=A(LISTA(J))+DA(J)
16  CONTINUE
  CHISQ0=CHISQ

  CALL MRQCOF(X,Y,SIG,NDATA,ATRY,MA,LISTA,MFIT,COVAR,DA,NCA,
*     CHISQ)

IF(CHISQ.LT.OCHISQ) THEN
C   SUCCESS, ACCEPT THE NEW SOLUTION.
  ALAMDA=0.1*ALAMDA
  OCHISQ=CHISQ
  DO 18 J=1, MFIT
    DO 17 K=1, MFIT
      ALPHA(J,K)=COVAR(J,K)
17    CONTINUE
      BETA(J)=DA(J)
      A(LISTA(J))=ATRY(LISTA(J))
18    CONTINUE
  ELSE
C   FAILURE, INCREASE ALAMDA AND RETURN.
  ALAMDA=10.*ALAMDA
  CHISQ=OCHISQ
ENDIF
PRINT *, 'ALAMDA=', ALAMDA
PRINT *, 'ERROR= ', CHISQ
RETURN
END

SUBROUTINE GAUSSJ(A,N,NP,B,M,MP)

```

```

PARAMETER (NMAX=50)
DIMENSION A(NP,NP),B(NP,MP),IPIV(NMAX),INDXR(NMAX),INDXC(NMAX)
C THE INTEGER ARRAYS IPIV,INDXR AND INDXC ARE USED FOR BOOKKEEPING
C ON THE PIVOTING. NMAX SHOULD BE AS LARGE AS THE LARGEST ANTICIPATED
C VALUE OF N.

DO 11 J=1,N
    IPIV(J)=0
11 CONTINUE
DO 22 I=1,N
C THIS IS THE MAIN LOOP OVER THE COLUMNS TO BE REDUCED.
    BIG=0
    DO 13 J=1,N
        IF(IPIV(J).NE.1) THEN
            DO 12 K=1,N
                IF(IPIV(K).EQ.0) THEN
                    IF(ABS(A(J,K)).GE.BIG) THEN
                        BIG=ABS(A(J,K))
                        IROW=J
                        ICOL=K
                    ENDIF
                    ELSE IF(IPIV(K).GT.1) THEN
                        PAUSE 'SINGULAR MATRIX'
                    ENDIF
12 CONTINUE
                ENDIF
13 CONTINUE
                IPIV(ICOL)=IPIV(ICOL)+1

C WE NOW HAVE THE PIVOT ELEMENT, SO WE INTERCHANGE ROWS, IF NEEDED,
C TO PUT THE PIVOT ELEMENT ON THE DIAGNAL. THE COLUMNS ARE NOT
C PHYSICALLY INTERCHANGED, ONLY RELABELED: INDX(I), THE COLUMN OF
C THE ITH PIVOT ELEMENT, IS THE ITH COLUMN THAT IS REDUCED, WHILE
C INDXR(I) IS THE ROW IN WHICH THAT PIVOT ELEMENT WAS ORIGINALLY
C LOCATED. IF INDXR(I) IS NOT EQUAL TO INDXC(I) THERE IS AN IMPLIED
C COLUMN INTERCHANGE. WITH THIS FORM OF BOOKKEEPING, THE SOLUTION B'S
C WILL END UP IN THE CORRECT ORDER, AND THE INVERSE MATRIX WILL BE
C SCRAMBLED BY COLUMNS.

                IF(IROW.NE.ICOL) THEN
                    DO 14 L=1,N
                        DUM=A(IROW,L)
                        A(IROW,L)=A(ICOL,L)
                        A(ICOL,L)=DUM
14 CONTINUE
                    DO 15 L=1,M
                        DUM=B(IROW,L)
                        B(IROW,L)=B(ICOL,L)
                        B(ICOL,L)=DUM
15 CONTINUE
                ENDIF

```

```

C      WE ARE NOW READY TO DIVIDE THE PIVOT ROW BY THE PIVOT ELEMENT,
C      LOCATED AT IROW AND ICOL.
      INDXR(I)=IROW
      INDXC(I)=ICOL
      IF(A(ICOL,ICOL).EQ.0) PAUSE 'SINGULAR MATRIX'
      PIVINV=1./A(ICOL,ICOL)
      A(ICOL,ICOL)=1.
      DO 16 L=1,N
        A(ICOL,L)=A(ICOL,L)*PIVINV
16     CONTINUE
      DO 17 L=1,M
        B(ICOL,L)=B(ICOL,L)*PIVINV
17     CONTINUE

C      NEXT, WE REDUCE THE ROWS, EXCEPT FOR THE PIVOT ONE, OF COURSE.
      DO 21 LL=1,N
        IF(LL.NE.ICOL) THEN
          DUM= A(LL,ICOL)
          A(LL,ICOL)=0
          DO 18 L=1,N
            A(LL,L)=A(LL,L)-A(ICOL,L)*DUM
18         CONTINUE
          DO 19 L=1,M
            B(LL,L)=B(LL,L)-B(ICOL,L)*DUM
19         CONTINUE
          ENDIF
21     CONTINUE
22     CONTINUE

C      IT REMAINS TO UNSCRAMBLE THE SOLUTION IN VIEW OF THE COLUMNS
C      INTERCHANGES. WE DO THIS BY INTERCHANGING PAIRS OF COLUMNS IN
C      THE REVERSE ORDER THAT THE PERMUTATION WAS BUILT UP.
      DO 24 L=N,1,-1
        IF(INDXR(L).NE.INDXC(L)) THEN
          DO 23 K=1,N
            DUM=A(K,INDXR(L))
            A(K,INDXR(L))=A(K,INDXC(L))
            A(K,INDXC(L))=DUM
23         CONTINUE
          ENDIF
24     CONTINUE
      RETURN
      END

      SUBROUTINE COVSRT(COVAR,NCVM,MA,LISTA,MFIT)

C      GIVEN THE COVARIANCE MATRIX COVAR OF A FIT FOR MFIT OF MA TOTAL
C      PARAMETERS, AND THEIR ORDERING LISTA(I), REPACK THE COVARIANCE MATRIX
C      TO THE TRUE ORDER OF THE PARAMETERS. ELEMENTS ASSOCIATED WITH FIXED
C      PARAMETERS WILL BE ZERO. NCVM IS THE PHYSICAL DIMENSION OF COVAR.

```

```

        DIMENSION COVAR(NCVM,NCVM),LISTA(MFIT)
        DO 12 J=1,MA-1
          DO 11 I=J+1,MA
            COVAR(I,J)=0
11          CONTINUE
12          CONTINUE

C      REPACK OFF-DIAGNAL ELEMENTS OF FIT INTO CORRECT LOCATIONS BELOW
C      DIAGNAL
        DO 14 I=1,MFIT-1
          DO 13 J=I+1,MFIT
            IF(LISTA(J).GT.LISTA(I)) THEN
              COVAR(LISTA(J),LISTA(I))=COVAR(I,J)
            ELSE
              COVAR(LISTA(I),LISTA(J))=COVAR(I,J)
            ENDIF
13          CONTINUE
14          CONTINUE

C      TEMPORARILLY STORE ORIGINAL DIAGONAL ELEMENTS IN TOP ROW, AND ZERO
C      THE DIAGONAL.
        SWAP=COVAR(1,1)
        DO 15 J=1,MA
          COVAR(1,J)=COVAR(J,J)
          COVAR(J,J)=0.
15          CONTINUE
        COVAR(LISTA(1),LISTA(1))=SWAP
C      SORT ELEMENTS INTO PROPER ORDER ON DIAGONAL.
        DO 16 J=2,MFIT
          COVAR(LISTA(J),LISTA(J))=COVAR(1,J)
16          CONTINUE
C      FILL IN ABOVE DIAGONAL BY SYMMETRY
        DO 18 J=2,MA
          DO 17 I=1,J-1
            COVAR(I,J)=COVAR(J,I)
17          CONTINUE
18          CONTINUE
        RETURN
        END

        SUBROUTINE MRQCOF(X,Y,SIG,NDATA,A,MA,LISTA,MFIT,ALPHA,BETA,NALP,
*          CHISQ)

C      USED BY MRQMIN TO EVALUATE THE LINEARIZED FITTING MATRIX ALPHA,
C      AND VECTOR BETA.

        PARAMETER(MMAX=20)
        DIMENSION X(NDATA),Y(NDATA),SIG(NDATA),ALPHA(NALP,NALP),
*          BETA(MA),DYDA(MMAX),LISTA(MFIT),A(MA)

```



```

DO 12 J=1,MFIT
  DO 11 K=1,J
    ALPHA(J,K)=0.
11  CONTINUE
    BETA(J)=0.
12  CONTINUE
  CHISQ=0.
  DO 15 I=1,NDATA
    CALL SINE(X(I),A,YMOD,DYDA,MA)
    SIG2I=1./(SIG(I)*SIG(I))
    DY=Y(I)-YMOD
    DO 14 J=1,MFIT
      WT=DYDA(LISTA(J))*SIG2I
      DO 13 K=1,J
        ALPHA(J,K)=ALPHA(J,K)+WT*DYDA(LISTA(K))
13      CONTINUE
        BETA(J)=BETA(J)+DY*WT
14      CONTINUE
      CHISQ=CHISQ+DY*DY*SIG2I
15  CONTINUE
  DO 17 J=2,MFIT
    DO 16 K=1,J-1
      ALPHA(K,J)=ALPHA(J,K)
16  CONTINUE
17  CONTINUE
  RETURN
  END

SUBROUTINE SINE(X,A,Y,DYDA,NA)
DIMENSION A(NA),DYDA(NA)
Y=0.
TPI=6.2831852
DO I=1,NA-1,3
  Y=Y+A(I)*SIN(TPI*A(I+1)*X+A(I+2))
  DYDA(I)=SIN(TPI*A(I+1)*X+A(I+2))
  DYDA(I+1)=A(I)*TPI*A(I+1)*COS(TPI*A(I+1)*X+A(I+2))
  DYDA(I+2)=A(I)*COS(TPI*A(I+1)*X+A(I+2))
ENDDO
RETURN
END

```

PROGRAM MEM

```

C      THIS PROGRAM IS USED TO ESTIMATE THE MAIN PERIODS HIDDEN
C      IN THE DENSITY VARIATION AT DIFFERENT ALTITUDES. GIVEN THE
C      LENGTH N OF THE INPUT DATA SEQUENCE AND THE NUMBERS OF
C      OF THE POLES M, THE PROGRAM PRODUCES THE ESTIMATED SPECTRUMS
C      AT THE SPECIFIED ALTITUDES.
C      INPUT:
C      DA4.DAT. THE FILE HAS 5 KM STEPS AND 9 LEVELS.
C      OUTPUT:
C      MA.DAT,...,MI.DAT

      DIMENSION DATA(50),WK1(50),WK2(50),WKM(50),COF(50)
      CHARACTER CHAR1*1,FILE*3

      PRINT *, 'ENTER THE NUMBER OF SAMPLES--N: (FOR LIDAR DATA,
1      N=22; FOR MAP-MF, N=18; FOR MAP-MD, N=
      READ *, N
      PRINT *, 'ENTER THE NUMBER OF POLES YOU WANT TO SPECIFY--M'
      READ *, M
      PRINT *, 'ENTER THE NUMBER OF LEVELS YOU SPECIFIED--LEVL. FOR
1      LIDAR DATA, LEVL=9; FOR MAP-WINE, LEVL=7.'
      READ *, LEVL
      PRINT *, 'ENTER THE NAME OF THE DATA FILE TO BE OPENED'
      ACCEPT 5, FILE
5      FORMAT(A)
      OPEN(UNIT=3, TYPE='OLD', NAME=FILE)
      DO 100 I=1, LEVL
          DO J=1, N
              READ(3, *) DATA(J)
              DATA(J)=DATA(J)
          ENDDO

          CALL MEMCOF(DATA, N, M, PM, COF, WK1, WK2, WKM)

          I1=I+64
          CHAR1=CHAR(I1)
          OPEN(UNIT=4, TYPE='NEW', NAME='M' // CHAR1)
          DO J=0, 200
              FDT=FLOAT(J)/400.
              Y=EVLMEM(FDT, COF, M, PM)
              WRITE(4, *) FDT, Y
          ENDDO
          CLOSE(4)
C      STOP
100     CONTINUE
        CLOSE(3)
        STOP
        END

C      The function of the subroutine is as following:
C      Given a real vector of DATA of length N, and given M, this routine

```

C returns a vector COF of length M with $\text{COF}(j)=a_j$, and a scalar $\text{PM}=b_0$,
 C which are the coefficients for Maximum Entropy Method spectral
 C estimation. The user must provide workspace vectors WK1, WK2 and
 C WKM of length N, N and M, respectively.

```

SUBROUTINE MEMCOF(DATA,N,M,PM,COF,WK1,WK2,WKM)
DIMENSION DATA(N),COF(M),WK1(N),WK2(N),WKM(M)
P=0.
DO J=1,N
  P=P+DATA(J)*DATA(J)
ENDDO
PM=P/N
WK1(1)=DATA(1)
WK2(N-1)=DATA(N)
DO J=2,N-1
  WK1(J)=DATA(J)
  WK2(J-1)=DATA(J)
ENDDO
DO 17 K=1,M
  PNEUM=0.
  DENOM=0.
  DO J=1,N-K
    PNEUM=PNEUM+WK1(J)*WK2(J)
    DENOM=DENOM+WK1(J)**2+WK2(J)**2
  ENDDO
  COF(K)=2.*PNEUM/DENOM
  PM=PM*(1.-COF(K)**2)
  IF(K.NE.1) THEN
    DO I=1,K-1
      COF(I)=WKM(I)-COF(K)*WKM(K-I)
    ENDDO
  ENDDO
ENDIF

```

C The algorithm is recursive, building up the answer for larger
 C and larger values of M until the desired value is reached. At
 C this point in the algorithm, one could return the vector COF
 C and scalar for an MEM spectral estimate of K (rather than M)
 C terms.

```

IF(K.EQ.M) RETURN
DO I=1,K
  WKM(I)=COF(I)
ENDDO
DO J=1,N-K-1
  WK1(J)=WK1(J)-WKM(K)*WK2(J)
  WK2(J)=WK2(J+1)-WKM(K)*WK1(J+1)
ENDDO
17 CONTINUE
PAUSE 'NEVER GET THERE'
END

```

C The following FUNCTION returns the power spectrum estimates P(f)
C as a function of FDT=f*delta.

```
FUNCTION EVLMEM(FDT,COF,M,PM)
DIMENSION COF(M)
REAL*8 WR,WI,WPR,WPI,WTEMP,THETA
THETA=6.28318530717959D0*FDT
WPR=DCOS(THETA)
WPI=DSIN(THETA)
WR=1.D0
WI=0.D0
SUMR=1.
SUMI=0.
DO 11 I=1,M
  WTEMP=WR
  WR=WR*WPR-WI*WPI
  WI=WI*WPR+WTEMP*WPI
  SUMR=SUMR-COF(I)*SGL(WR)
  SUMI=SUMI-COF(I)*SGL(WI)
11 ENDDO
EVLMEM=PM/(SUMR**2+SUMI**2)
RETURN
END
```

PROGRAM PICK5

C THIS PROGRAM IS USED TO LIFT THE DENSITY RATIO FROM THE
 C THE ORIGINAL DATA FILES WITH THE RESOLUTION OF 1KM AND
 C THEN DO THE INTERPOLATIONS.
 C INPUT:
 C SAME AS THOSE IN 'PICK.FOR'.
 C OUTPUT:
 C 1. DA5.DAT. DATA FILE CONTAINS THE DENSITIES AT DIFFERENT
 C ALTITUDES (1 KM RESOLUTION) WITH AVERAGES BEING SUBTRACTED.
 C 2. AVER.DAT. THE FILE THAT CONTAINS THE AVERAGE DENSITIES AT
 C DIFFERENT ALTTIODES.

```

REAL DEN(50,30),ALT(250),RDEN(250),FDEN(250),RATIO(250),
1 SGMA(250),TEMP(250),SNR(250),Y(50,30),AVER(50)
INTEGER NUM(250),NF(250)
CHARACTER FILE*15,PRE(9)*80, CI*1,CHAR1*1
  
```

C READ THE DENSITY RATIOS AT THE ALTITUDES FROM 25 THROUGH 65KM.

```

N1=19
DO 200 I=65,65+N1-1
  L=I-64
  CI=CHAR(I)
  FILE='gf'//CI//'.DEN'
  PRINT *,FILE
  OPEN(UNIT=3,TYPE='OLD',NAME=FILE)
C READ THE TOP OF THE DATA FILES
  DO J=1,9
    READ(3,10) PRE(J)
10  FORMAT(A)
    ENDDO
    K=1
    LA=25
    DO J=1,170
      READ(3,*) NUM(J),ALT(J),RDEN(J),FDEN(J),RATIO(J),
1      SGMA(J), NF(J),TEMP(J),SNR(J)
      ENDDO
      DO 100 J=1,200
        IF(INT(ALT(J)+0.2).EQ.LA) THEN
          DEN(K,L)=RATIO(J)
          LA=LA+1
          PRINT *, ALT(J),K,L,DEN(K,L)
          K=K+1
        ENDIF
        IF(LA.GT.65) GOTO 200
100  CONTINUE
200  CONTINUE
      CLOSE(3)
      PRINT*, 'THE LEVELS K=',K

N=N1
  
```

```

LEVL=K

DO I=1,LEVL
  K=0
  DO J=1,N
    IF(J.EQ.5) THEN
      Y(I,J+K)=DEN(I,J)
      K=K+1
      Y(I,J+K)=(DEN(I,J)+DEN(I,J+1))/2.
    ELSE IF(J.EQ.12) THEN
      Y(I,J+K)=DEN(I,J)
      K=K+1
      Y(I,J+K)=2*(DEN(I,J)-DEN(I,J-1))+DEN(I,J-1)
      K=K+1
      Y(I,J+K)=-2*(DEN(I,J+3)-DEN(I,J+4))+DEN(I,J+3)
    ELSE
      Y(I,J+K)=DEN(I,J)
    ENDIF
  ENDDO
ENDDO
N=N+K
PRINT *, 'NEW N=', N

OPEN(UNIT=6,TYPE='NEW',NAME='AVER')
OPEN(UNIT=4,TYPE='NEW',NAME='DA5')
DO I=1,LEVL
  SUM=0.
  DO K=1,N9
    SUM=SUM+Y(I,K)
  ENDDO
  AVER(I)=SUM/N
  WRITE(6,*) AVER(I)
  PRINT *, 'AVER=', AVER(I)
  DO K=1,N
    WRITE(4,*) Y(I,K)-AVER(I)
  ENDDO
ENDDO
CLOSE(4)
CLOSE(6)
PRINT*, 'DO YOU WANT TO CREATE DATA FILES TO DRAW THE DENSITY
1 1 PROFILES AT DIFFERENT ALTITUDES ? ENTER Y OR N.'
ACCEPT 300, CHAR1
300 FORMAT(A1)
IF(CHAR1.EQ.'Y'.OR.CHAR1.EQ.'y') THEN
  OPEN(UNIT=4,TYPE='NEW',NAME='LEVL')
  DO I=1,LEVL
    DO L=1,N
      WRITE(6,*) Y(I,L)-AVER(I)
    ENDDO
  ENDDO
  CLOSE(4)
ENDIF

```

STOP
END

```

PROGRAM GSP

C      THIS PROGRAM IS USED TO GENERATE GRAVITY WAVE SIGNALS BY
C      FILTERING OUT THE LOW FREQUENCY COMPONENTS FROM THE DAILY
C      DENSITY PROFILES. THE DAILY DENSITY PROFILES ARE SIMULATED
C      BY LSE MODELS.
C      USE 'LINK GSP,@SYS:IMSL' TO CONNECT 'RCURV' TO THIS PROGRAM.
C      INPUT:
C          ORIGINAL 5-MINUTE PROFILES.
C      OUTPUT:
C          GSP.DAT. FILE CONTAINS THE DENSITY VARIATIONS CAUSED BY
C              GRAVITY WAVES.
C          LSE.DAT. FILE CONTAINS THE RESULT OF LSE SIMULATION OF
C              THE DAILY DENSITY PROFILES.
C          RATIO.DAT. FILE CONTAINS THE MEASURED DAILY DENSITY PROFILE.

      REAL ALT(1000),RDEN(1000),FDEN(1000),RATIO(1000),Z(1000),
1      SGMA(1000),TEMP(1000),SNR(0:1000),DEN(1000),DENM(1000)
      INTEGER NUM(1000),NF(1000)
      REAL B(10),SSPOLY(10),STAT(10)
      REAL RWKSP(7100)
      CHARACTER FILE*15,PRE(9)*80, CI*1
      EXTERNAL RCURV
      COMMON /WORKSP/ RWKSP

C      READ THE DENSITY PROFILES.
      PRINT*,'ENTER NAME OF DATA FILE TO BE PROCESSED,e.g.,1805'
      ACCEPT 10,FILE
      PRINT *,'G602'//FILE//'.den'
      OPEN(UNIT=3,TYPE='OLD',NAME='G602'//FILE//'.den')
C      READ THE TOP OF THE DATA FILES
      DO J=1,9
10      READ(3,10) PRE(J)
          FORMAT(A)
      ENDDO
      J=0
      SNR(J)=1000
      DO WHILE(SNR(J).NE.-999.0)
          J=J+1
          READ(3,*) NUM(J),ALT(J),RDEN(J),FDEN(J),RATIO(J),
1          SGMA(J), NF(J),TEMP(J),SNR(J)
      ENDDO
      N=J
      CLOSE(3)
      DO I=1,N
          Z(I)=ALT(I)/100.
      ENDDO
      DO J=1,10
          B(J)=0.
      ENDDO
      PRINT*,'ENTER THE DEGREE OF POLYN. NP='

```



```

READ* , NP
CALL RCURV(N,Z,RATIO,NP,B,SSPOLY,STAT)
DO I=1,N
  CALL FNT(I,Z(I),B,DENM(I))
  DEN(I)=RATIO(I)-DENM(I)
ENDDO
PRINT* , 'ENTER THE RANGE OF THE ALTITUDE M: M=30 IF 25-45 KM'
PRINT* , 'M=63 IF 35-55 KM, M=96 IF 45-65KM'
READ* , M
ML=64
OPEN(4,TYPE='NEW',NAME='GSP')
DO I=1,ML
  WRITE(4,*)DEN(I+M)
ENDDO
CLOSE(4)
OPEN(4,TYPE='NEW',NAME='LSE')
DO I=1,ML
  WRITE(4,*) DENM(I+M),ALT(I+M)
ENDDO
CLOSE(4)
OPEN(4,TYPE='NEW',NAME='RATIO')
DO I=1,N
  WRITE(4,*) RATIO(I),ALT(I)
ENDDO
CLOSE(4)
STOP
END

```

C DEFINE A POLYNOMIAL WHICH WILL SIMULATE THE DENSITY CURVE.

```

SUBROUTINE FNT(I,X,B,DENM)
REAL B(10)
DENM=B(1)
DO J=2,10
  DENM=DENM+B(J)*X**(J-1)
ENDDO
RETURN
END

```

PROGRAM PDM

C THIS PROGRAM IS USED TO ESTIMATE THE SPECTRUMS OF PLANETARY
 C WAVES AT DIFFERENT ALTITUDES OR THE SPECTRUMS OF GRAVITY WAVES
 C INPUT:
 C DA6.DAT. (FILE CONTAINS THE DENSITY SIGNALS WITH LENGTH 44.)
 C OR GSP.DAT. (FILE CONTAINS THE DIFFERENCE BETWEEN THE MEASURED
 C DENSITIES AND THE LSE MODELED ONES.N=64)
 C OUTPUT:
 C PPD.M.DAT. FILE CONTAINS THE SPECTRUMS OF PLANETARY WAVES.
 C PDM.DAT FILE CONTAINS THE SPECTRUMS OF GRAVITY WAVES.

REAL*8 A(2048),R(2048),b(2048),PI,AMP,F
 DOUBLE COMPLEX X(2048)
 CHARACTER*10 FILE,A1

PRINT *, 'ENTER THE NUMBER OF SAMPLES--N. IF THE INPUT IS DA6.DAT,
 1 N=44; IF THE INPUT IS GSP.DAT,N=64.'
 READ *, N

PRINT*, 'ENTER NAME OF DATA FILE TO BE OPENED: GSP OR DA6'
 ACCEPT 10,FILE
 10 FORMAT(A)
 IF(FILE.EQ. 'DA6'.OR.FILE.EQ. 'da6') THEN
 LEVEL=9
 ELSE
 LEVEL=1
 ENDIF
 PRINT *, 'ENTER THE SAMPLING INTERVAL.FOR DA6.DAT,DELTA=.5; FOR
 1 GSP.DAT,DELTA=.3.'
 READ *, DELTA

OPEN(UNIT=11,NAME=FILE,STATUS='OLD')
 DO 100 J=1,LEVEL
 DO L=1,2048
 R(L)=0.
 ENDDO
 READ(11,*) (A(I),I=1,N)
 C FIND THE ESTIMATION OF THE AUTOCORRELATIONS.
 DO K=1,N
 R(K)=0.
 DO I=1,N-K+1
 R(K)=R(K)+A(I+K-1)*A(I)
 ENDDO
 R(K)=R(K)/FLOAT(N)
 ENDDO
 C
 CHECK IF N=2**K
 I=1
 N0=N-2**I
 DO WHILE (N0.GT.0)

```
        I=I+1
        N0=N-2**I
        ENDDO
        N1=2**I
PRINT* , 'N1=' ,N1
        CALL FFTRC(R,N1,X,IWK,WK)
        OPEN(UNIT=4,STATUS='NEW',NAME='PDM')
        DO K=1,N1/2
            FR=FLOAT(K-1)/(N1*DELTA)
            AMP=CDABS(X(K))
            WRITE(4,*) FR,AMP
        ENDDO
        CLOSE(4)
100  CONTINUE
      CLOSE(11)
      STOP
      END
```